

AG
T

*Algebraic & Geometric
Topology*

Volume 23 (2023)

**A uniformizable spherical CR structure
on a two-cusped hyperbolic 3-manifold**

YUEPING JIANG

JIEYAN WANG

BAOHUA XIE



A uniformizable spherical CR structure on a two-cusped hyperbolic 3–manifold

YUEPING JIANG

JIEYAN WANG

BAOHUA XIE

Let $\langle I_1, I_2, I_3 \rangle$ be the complex hyperbolic $(4, 4, \infty)$ triangle group. We prove Schwartz’s conjecture that $\langle I_1, I_2, I_3 \rangle$ is discrete and faithful if and only if $I_1 I_3 I_2 I_3$ is nonelliptic. If $I_1 I_3 I_2 I_3$ is parabolic, we show that the even subgroup $\langle I_2 I_3, I_2 I_1 \rangle$ is the holonomy representation of a uniformizable spherical CR structure on the two-cusped hyperbolic 3–manifold $s782$ in SnapPy notation.

20H10, 22E40, 51M10, 57M50

1 Introduction

Let $\mathbb{H}_{\mathbb{C}}^2$ be the complex hyperbolic plane and $\mathrm{PU}(2, 1)$ be its holomorphic isometry group; see Section 2 for more details. It is well known that $\mathbb{H}_{\mathbb{C}}^2$ is one of the rank-one symmetric spaces and $\mathrm{PU}(2, 1)$ is a semisimple Lie group. $\mathbb{H}_{\mathbb{C}}^2$ can be viewed as the unit ball in \mathbb{C}^2 equipped with the Bergman metric. Its ideal boundary $\partial\mathbb{H}_{\mathbb{C}}^2$ is the 3–sphere S^3 . We study the geometry of discrete subgroups of $\mathrm{PU}(2, 1)$.

Let M be a 3–manifold. A *spherical CR structure* on M is a system of coordinate charts into S^3 such that the transition functions are restrictions of elements of $\mathrm{PU}(2, 1)$. Any spherical CR structure on M determines a pair (ρ, d) , where $\rho: \pi_1(M) \rightarrow \mathrm{PU}(2, 1)$ is the holonomy and $d: \tilde{M} \rightarrow S^3$ is the developing map. There is a special spherical CR structure. A *uniformizable spherical CR structure* on M is a homeomorphism between M and a quotient space Ω/Γ , where Γ is a discrete subgroup of $\mathrm{PU}(2, 1)$ and $\Omega \subset \partial\mathbb{H}_{\mathbb{C}}^2$ is the discontinuity region of Γ . An interesting problem in complex hyperbolic geometry is to find (uniformizable) spherical CR structures on hyperbolic 3–manifolds.

Geometric structures modeled on the boundary of complex hyperbolic space are rather difficult to construct. The first example of a spherical CR structure existing on a cusped

hyperbolic 3–manifold was discovered by Schwartz. In [23], Schwartz constructed a uniformizable spherical CR structure on the Whitehead link complement. He also constructed a closed hyperbolic 3–manifold that admits a uniformizable spherical CR structure in [26] at almost the same time.

Let M_8 be the complement of the figure eight knot. In [9], Falbel constructed two different representations ρ_1 and ρ_2 of $\pi_1(M_8)$ in $\text{PU}(2, 1)$, and proved that ρ_1 is the holonomy of a spherical CR structure on M_8 . In [11], Falbel and Wang proved that ρ_2 is also the holonomy of a spherical CR structure on M_8 . In [7], Deraux and Falbel constructed a uniformizable spherical CR structure on M_8 whose holonomy is ρ_2 . In [6], Deraux proved that there is a 1–parameter family of spherical CR uniformizations of the figure eight knot complement. This family is in fact a deformation of the uniformization constructed in [7].

Let us return to the Whitehead link complement. It admits a uniformizable spherical CR structure which is different from Schwartz's. In the recent work [22], Parker and Will also constructed a spherical CR uniformization of the Whitehead link complement. By applying spherical CR Dehn surgery theorems to the uniformizations of the Whitehead link complement, one can get infinitely many manifolds which admit uniformizable spherical CR structures. In [28], Schwartz proved a spherical CR Dehn surgery theorem, and applied it to the spherical CR uniformization of the Whitehead link complement constructed in [23] to obtain infinitely many closed hyperbolic 3–manifolds which admit uniformizable spherical CR structures. In [2], Acosta applied the spherical CR Dehn surgery theorem he proved in [1] to the spherical CR uniformization of the Whitehead link complement constructed by Parker and Will in [22] to obtain infinitely many one-cusped hyperbolic 3–manifolds which admit uniformizable spherical CR structures. In particular, the spherical CR uniformization of the complement of the figure eight knot constructed by Deraux and Falbel [7] is contained in this family.

There are some hyperbolic 3–manifolds described in the SnapPy census (see [4]) which admit spherical CR structures. In [5], Deraux proved that the cusped hyperbolic 3–manifold $m009$ admits a uniformizable spherical CR structure whose holonomy representation was constructed by Falbel, Koseleff and Rouillier in [10]. In [16; 18], Ma and Xie proved that the cusped hyperbolic 3–manifolds $m038$, $s090$, $m295$ and 6_1^3 admit spherical CR uniformizations. They also gave the second explicit example of a closed hyperbolic 3–orbifold which admits a uniformizable spherical CR structure in [17].

We show that the two-cusped hyperbolic 3–manifold $s782$ admits a uniformizable spherical CR structure. By studying the action of the even subgroup of a discrete

complex hyperbolic triangle group on $\mathbb{H}_{\mathbb{C}}^2$, we prove that the quotient space of its discontinuity region is homeomorphic to $s782$. That means the holonomy representation of the spherical CR uniformization of $s782$ is a triangle group.

Now let us talk about the complex hyperbolic triangle groups. Let $\Delta_{p,q,r}$ be the abstract (p, q, r) reflection triangle group with the presentation

$$\langle \sigma_1, \sigma_2, \sigma_3 \mid \sigma_1^2 = \sigma_2^2 = \sigma_3^2 = (\sigma_2\sigma_3)^p = (\sigma_3\sigma_1)^q = (\sigma_1\sigma_2)^r = \text{id} \rangle,$$

where p, q and r are positive integers, or ∞ in which case the corresponding relation disappears. A *complex hyperbolic (p, q, r) triangle group* is a representation of $\Delta_{p,q,r}$ in $\text{PU}(2, 1)$, which maps the generators to complex involutions fixing complex lines in $\mathbb{H}_{\mathbb{C}}^2$. The study of complex hyperbolic triangle groups was begun by Goldman and Parker, and in [13] they studied the complex hyperbolic (∞, ∞, ∞) triangle groups. They conjectured that a representation of $\Delta_{\infty,\infty,\infty}$ into $\text{PU}(2, 1)$ is discrete and faithful if and only if the image of $\sigma_1\sigma_2\sigma_3$ is nonelliptic. The Goldman–Parker conjecture was proved by Schwartz in [24] (and with a better proof in [27]). In particular, the representation with the image of $\sigma_1\sigma_2\sigma_3$ being parabolic is closely related with the holonomy of the spherical CR uniformization of the Whitehead link complement constructed in [23]. In the survey [25], a series of conjectures on complex hyperbolic triangle groups are put forward.

Conjecture 1.1 (Schwartz [25]) *Suppose that $p \leq q \leq r$. Let $\langle I_1, I_2, I_3 \rangle$ be a complex hyperbolic (p, q, r) triangle group. Then $\langle I_1, I_2, I_3 \rangle$ is a discrete and faithful representation of $\Delta_{p,q,r}$ if and only if $I_1I_3I_2I_3$ and $I_1I_2I_3$ are nonelliptic. Moreover:*

- *If $3 \leq p < 10$, then $\langle I_1, I_2, I_3 \rangle$ is discrete and faithful if and only if $I_1I_3I_2I_3$ is nonelliptic.*
- *If $p > 13$, then $\langle I_1, I_2, I_3 \rangle$ is discrete and faithful if and only if $I_1I_2I_3$ is nonelliptic.*

In a recent work [22], Parker and Will proved Conjecture 1.1 for complex hyperbolic $(3, 3, \infty)$ groups. They also showed that, when $I_1I_3I_2I_3$ is parabolic, the quotient of $\mathbb{H}_{\mathbb{C}}^2$ by the group $\langle I_2I_3, I_2I_1 \rangle$ is a complex hyperbolic orbifold whose boundary is a spherical CR uniformization of the Whitehead link complement. In [21], Parker, Wang and Xie proved Conjecture 1.1 for complex hyperbolic $(3, 3, n)$ groups with $n \geq 4$. Furthermore, Acosta [2] showed that when $I_1I_3I_2I_3$ is parabolic the group $\langle I_2I_3, I_2I_1 \rangle$ is the holonomy representation of a uniformizable spherical CR structure on the Dehn surgery of the Whitehead link complement on one cusp of type $(1, n - 3)$.

We give a proof of Conjecture 1.1 for the complex hyperbolic $(4, 4, \infty)$ triangle groups and further analyze the group when $I_1 I_3 I_2 I_3$ is parabolic. Our result is as follows:

Theorem 1.2 *Let $\langle I_1, I_2, I_3 \rangle$ be a complex hyperbolic $(4, 4, \infty)$ triangle group. Then $\langle I_1, I_2, I_3 \rangle$ is a discrete and faithful representation of $\Delta_{4,4,\infty}$ if and only if $I_1 I_3 I_2 I_3$ is nonelliptic. Moreover, when $I_1 I_3 I_2 I_3$ is parabolic, the quotient of $\mathbb{H}_{\mathbb{C}}^2$ by the group $\langle I_2 I_3, I_2 I_1 \rangle$ is a complex hyperbolic orbifold whose boundary is a spherical CR uniformization of the two-cusped hyperbolic 3-manifold $s782$ in the SnapPy census.*

In [29], Wyss-Gallifent studied the complex hyperbolic $(4, 4, \infty)$ triangle groups. He discovered several discrete groups with $I_1 I_3 I_2 I_3$ being regular elliptic of finite order and conjectured that there should be countably infinitely many. It would be very interesting to know what the manifold at infinity is for the group with $I_1 I_3 I_2 I_3$ being regular elliptic of finite order.

Our method is to construct Ford domains for the triangle groups acting on $\mathbb{H}_{\mathbb{C}}^2$. The space of complex hyperbolic $(4, 4, \infty)$ triangle groups $\langle I_1, I_2, I_3 \rangle$ is parametrized by the angle $\theta \in [0, \frac{\pi}{2})$; see Section 3. Let $S = I_2 I_3$, $T = I_2 I_1$ and $\Gamma = \langle S, T \rangle$. Here S is regular elliptic of order 4, and T is parabolic fixing the point at infinity. For each group in the parameter space, the Ford domain D is the intersection of the closures of the exteriors of the isometric spheres for the elements $S, S^{-1}, S^2, (S^{-1}T)^2$ and their conjugations by the powers of T . The combination of D is the same except when $I_1 I_3 I_2 I_3$ is parabolic, in which case there are additional parabolic fixed points. D is preserved by the subgroup $\langle T \rangle$ and is a fundamental domain for the cosets of $\langle T \rangle$ in Γ . Its ideal boundary $\partial_{\infty} D$ is the complement of a tubular neighborhood of the T -invariant \mathbb{R} -circle (or horotube defined in [28]). By intersecting $\partial_{\infty} D$ with a fundamental domain for $\langle T \rangle$ acting on $\partial \mathbb{H}_{\mathbb{C}}^2$, we obtain a fundamental domain for Γ acting on its discontinuity region; see Section 4.

When $I_1 I_3 I_2 I_3$ is parabolic, that is $\theta = \frac{\pi}{3}$, there are four additional parabolic fixed points fixed by $T^{-1} S^2, S^2 T^{-1}, S T^{-1} S$ and $T^{-1} S T^{-1} S T$, except the point at infinity which is the fixed point of T ; see Section 5. By studying the combinatorial properties of the fundamental domain for Γ acting on its discontinuity region $\Omega(\Gamma)$, we prove that the quotient $\Omega(\Gamma)/\Gamma$ is homeomorphic to the two-cusped hyperbolic 3-manifold $s782$. Motivated by the work of Acosta [2], we guess that there are similar structures on its surgeries.

Acknowledgments We thank Jiming Ma for his help in the proof of Theorem 5.22. Xie also would like to thank Jiming Ma for numerous helpful discussions on complex

hyperbolic geometry during his visit to Fudan University. We would like to thank the referee for comments which improved a previous version of this paper. Jiang was supported by NSFC 12271148. Wang was supported by NSFC 11701165. Xie was supported by NSFC 11871202 and Hunan Provincial Natural Science Foundation of China 2018JJ3024.

2 Background

The purpose of this section is to briefly introduce complex hyperbolic geometry. One can refer to Goldman’s book [12] for more details.

2.1 Complex hyperbolic plane

Let $\langle z, w \rangle = w^* H z$ be the Hermitian form on \mathbb{C}^3 associated to H , where H is the Hermitian matrix

$$H = \begin{bmatrix} 0 & 0 & 1 \\ 0 & 1 & 0 \\ 1 & 0 & 0 \end{bmatrix}.$$

Then \mathbb{C}^3 is the union of the negative cone V_- , null cone V_0 and positive cone V_+ , where

$$V_- = \{z \in \mathbb{C}^3 - \{0\} : \langle z, z \rangle < 0\}, \quad V_0 = \{z \in \mathbb{C}^3 - \{0\} : \langle z, z \rangle = 0\},$$

and

$$V_+ = \{z \in \mathbb{C}^3 - \{0\} : \langle z, z \rangle > 0\}.$$

Definition 2.1 Let $P: \mathbb{C}^3 - \{0\} \rightarrow \mathbb{C}P^2$ be the projectivization map. Then the *complex hyperbolic plane* $\mathbb{H}_{\mathbb{C}}^2$ is defined to be $P(V_-)$, and its boundary $\partial\mathbb{H}_{\mathbb{C}}^2$ is defined to be $P(V_0)$. This is the *Siegel domain model* of $\mathbb{H}_{\mathbb{C}}^2$.

There is another model of $\mathbb{H}_{\mathbb{C}}^2$.

Definition 2.2 The *ball model* of $\mathbb{H}_{\mathbb{C}}^2$ is the unit ball in \mathbb{C}^2 , which is given by the Hermitian matrix $J = \text{diag}(1, 1, -1)$. In this model, $\partial\mathbb{H}_{\mathbb{C}}^2$ is then the 3-dimensional sphere $S^3 \subset \mathbb{C}^2$. The *Cayley transform* C is given by

$$C = \frac{1}{\sqrt{2}} \begin{pmatrix} 1 & 0 & 1 \\ 0 & \sqrt{2} & 0 \\ 1 & 0 & -1 \end{pmatrix}.$$

It satisfies $C^* H C = J$ and interchanges the Siegel domain model and the ball model of $\mathbb{H}_{\mathbb{C}}^2$.

Let $\mathcal{N} = \mathbb{C} \times \mathbb{R}$ be the Heisenberg group with product

$$[z, t] \cdot [\zeta, v] = [z + \zeta, t + v - 2 \operatorname{Im}(\bar{z}\zeta)].$$

Then, in the Siegel domain model of $\mathbb{H}_{\mathbb{C}}^2$, the boundary of the complex hyperbolic plane $\partial\mathbb{H}_{\mathbb{C}}^2$ can be identified to the union $\mathcal{N} \cup \{q_{\infty}\}$, where q_{∞} is the point at infinity. The *standard lift* of q_{∞} and $q = [z, t] \in \mathcal{N}$ in \mathbb{C}^3 are

$$(2-1) \quad \mathbf{q}_{\infty} = \begin{bmatrix} 1 \\ 0 \\ 0 \end{bmatrix} \quad \text{and} \quad \mathbf{q} = \begin{bmatrix} \frac{1}{2}(-|z|^2 + it) \\ z \\ 1 \end{bmatrix}.$$

The closure of the complex hyperbolic plane $\mathbb{H}_{\mathbb{C}}^2 \cup \partial\mathbb{H}_{\mathbb{C}}^2$ can be identified to the union of $\mathcal{N} \times \mathbb{R}_{\geq 0}$ and $\{q_{\infty}\}$. Any point $q = (z, t, u) \in \mathcal{N} \times \mathbb{R}_{\geq 0}$ has the standard lift

$$\mathbf{q} = \begin{bmatrix} \frac{1}{2}(-|z|^2 - u + it) \\ z \\ 1 \end{bmatrix}.$$

Here (z, t, u) is called the *horospherical coordinates* of $\mathbb{H}_{\mathbb{C}}^2 \cup \partial\mathbb{H}_{\mathbb{C}}^2$. Let $d(u, v)$ be the distance between two points $u, v \in \mathbb{H}_{\mathbb{C}}^2$. Then the *Bergman metric* on the complex hyperbolic plane is given by the distance formula

$$\cosh^2\left(\frac{1}{2}d(u, v)\right) = \frac{\langle \mathbf{u}, \mathbf{v} \rangle \langle \mathbf{v}, \mathbf{u} \rangle}{\langle \mathbf{u}, \mathbf{u} \rangle \langle \mathbf{v}, \mathbf{v} \rangle},$$

where $\mathbf{u}, \mathbf{v} \in \mathbb{C}^3$ are lifts of u and v .

Definition 2.3 The *Cygan metric* d_{Cyg} on $\partial\mathbb{H}_{\mathbb{C}}^2 - \{q_{\infty}\}$ is defined to be

$$(2-2) \quad d_{\text{Cyg}}(p, q) = |2\langle \mathbf{p}, \mathbf{q} \rangle|^{1/2} = \left| |z - w|^2 - i(t - s + 2 \operatorname{Im}(z\bar{w})) \right|^{1/2},$$

where $p = [z, t]$ and $q = [w, s]$.

The Cygan metric satisfies the properties of a distance. The *extended Cygan metric* on $\mathbb{H}_{\mathbb{C}}^2$ is given by the formula

$$(2-3) \quad d_{\text{Cyg}}(p, q) = \left| |z - w|^2 + |u - v| - i(t - s + 2 \operatorname{Im}(z\bar{w})) \right|^{1/2},$$

where $p = (z, t, u)$ and $q = (w, s, v)$.

The formula $d_{\text{Cyg}}(p, q) = |2\langle \mathbf{p}, \mathbf{q} \rangle|^{1/2}$ remains valid even if one of p or q lies on $\partial\mathbb{H}_{\mathbb{C}}^2$. A *Cygan sphere* is a sphere for the extended Cygan distance.

There are two kinds of 2-dimensional totally real totally geodesic subspaces of $\mathbb{H}_{\mathbb{C}}^2$: complex lines and Lagrangian planes.

Definition 2.4 Let v^\perp be the orthogonal space of $v \in V_+$ with respect to the Hermitian form. The intersection of the projective line $P(v^\perp)$ with $\mathbb{H}_\mathbb{C}^2$ is called a *complex line*. The vector v is its *polar vector*.

The ideal boundary of a complex line on $\partial\mathbb{H}_\mathbb{C}^2$ is called a \mathbb{C} -circle. In the Heisenberg group, \mathbb{C} -circles are either vertical lines or ellipses whose projections on the z -plane are circles.

Let $\mathbb{H}_\mathbb{R}^2 = \{(x_1, x_2) \in \mathbb{H}_\mathbb{C}^2 : x_1, x_2 \in \mathbb{R}\}$ be the set of real points. $\mathbb{H}_\mathbb{R}^2$ is a Lagrangian plane. All the Lagrangian planes are the images of $\mathbb{H}_\mathbb{R}^2$ by isometries of $\mathbb{H}_\mathbb{C}^2$. The ideal boundary of a Lagrangian plane is called an \mathbb{R} -circle. In the Heisenberg group, \mathbb{R} -circles are either straight lines or lemniscate curves whose projections on the z -plane are the figure eight.

2.2 Isometries

Let $SU(2, 1)$ be the special unitary matrix preserving the Hermitian form. Then the projective unitary group $PU(2, 1) = SU(2, 1)/\{I, \omega I, \omega^2 I\}$ is the holomorphic isometry group of $\mathbb{H}_\mathbb{C}^2$, where $\omega = \frac{1}{2}(-1 + i\sqrt{3})$ is a primitive cubic root of unity. Note that complex conjugation also preserves the Bergman distance, and the full isometry group of $\mathbb{H}_\mathbb{C}^2$ is generated by $PU(2, 1)$ and complex conjugation; see Section 3.4 of [20].

Definition 2.5 Any isometry $g \in PU(2, 1)$ is *loxodromic* if it has exactly two fixed points on $\partial\mathbb{H}_\mathbb{C}^2$, *parabolic* if it has exactly one fixed point on $\partial\mathbb{H}_\mathbb{C}^2$, and *elliptic* if it has at least one fixed point in $\mathbb{H}_\mathbb{C}^2$.

The types of isometries can be determined by the traces of their matrix realizations; see Theorem 6.2.4 of Goldman [12]. Now suppose that $A \in SU(2, 1)$ has real trace. Then A is elliptic if $-1 \leq \text{tr}(A) < 3$. Moreover, A is unipotent if A is not the identity and $\text{tr}(A) = 3$. In particular, if $\text{tr}(A) = -1, 0, 1$, A is elliptic of order 2, 3 or 4, respectively.

There is a special class of elliptic elements of order two:

Definition 2.6 The *complex involution* on complex line C with polar vector n is

$$(2-4) \quad I_C(z) = -z + \frac{2\langle z, n \rangle}{\langle n, n \rangle} n.$$

It is obvious that I_C is a holomorphic isometry fixing the complex line C .

There is a special class of unipotent elements in $PU(2, 1)$:

Definition 2.7 A left Heisenberg translation associated to $[z, t] \in \mathcal{N}$ is given by

$$(2-5) \quad T_{[z,t]} = \begin{bmatrix} 1 & -\bar{z} & \frac{1}{2}(-|z|^2 + it) \\ 0 & 1 & z \\ 0 & 0 & 1 \end{bmatrix}.$$

It is obvious that $T_{[z,t]}$ fixes q_∞ and maps $[0, 0] \in \mathcal{N}$ to $[z, t]$.

2.3 Isometric spheres and Ford polyhedron

Suppose that $g = (g_{ij})_{i,j=1}^3 \in PU(2, 1)$ does not fix q_∞ . Then it is obvious that $g_{31} \neq 0$. We first recall the definition of isometric spheres and relevant properties; see for instance [20].

Definition 2.8 The isometric sphere of g , denoted by $\mathcal{I}(g)$, is the set

$$(2-6) \quad \mathcal{I}(g) = \{p \in \mathbb{H}_{\mathbb{C}}^2 \cup \partial\mathbb{H}_{\mathbb{C}}^2 : |\langle p, q_\infty \rangle| = |\langle p, g^{-1}(q_\infty) \rangle|\}.$$

The isometric sphere $\mathcal{I}(g)$ is the Cygan sphere with center

$$g^{-1}(q_\infty) = [\bar{g}_{32}/\bar{g}_{31}, 2 \operatorname{Im}(\bar{g}_{33}/\bar{g}_{31})]$$

and radius $r_g = \sqrt{2/|g_{31}|}$.

The interior of $\mathcal{I}(g)$ is the set

$$(2-7) \quad \{p \in \mathbb{H}_{\mathbb{C}}^2 \cup \partial\mathbb{H}_{\mathbb{C}}^2 : |\langle p, q_\infty \rangle| > |\langle p, g^{-1}(q_\infty) \rangle|\}.$$

The exterior of $\mathcal{I}(g)$ is the set

$$(2-8) \quad \{p \in \mathbb{H}_{\mathbb{C}}^2 \cup \partial\mathbb{H}_{\mathbb{C}}^2 : |\langle p, q_\infty \rangle| < |\langle p, g^{-1}(q_\infty) \rangle|\}.$$

The isometric spheres are paired as follows:

Lemma 2.9 [12, Section 5.4.5] *Let g be an element in $PU(2, 1)$ which does not fix q_∞ . Then g maps $\mathcal{I}(g)$ to $\mathcal{I}(g^{-1})$ and the exterior of $\mathcal{I}(g)$ to the interior of $\mathcal{I}(g^{-1})$. Also, for any unipotent transformation $h \in PU(2, 1)$ fixing q_∞ , we have $\mathcal{I}(g) = \mathcal{I}(hg)$.*

Since isometric spheres are Cygan spheres, we now recall some facts about Cygan spheres. Let $S_{[0,0]}(r)$ be the Cygan sphere with center $[0, 0]$ and radius $r > 0$. Then

$$(2-9) \quad S_{[0,0]}(r) = \{(z, t, u) \in \mathbb{H}_{\mathbb{C}}^2 \cup \partial\mathbb{H}_{\mathbb{C}}^2 : (|z|^2 + u)^2 + t^2 = r^4\}.$$

The geographical coordinates on the Cygan sphere will play an important role in our calculation; see Section 2.5 of [22].

Definition 2.10 The point $q = q(\alpha, \beta, w) \in S_{[0,0]}(r)$ with *geographical coordinates* (α, β, w) is the point whose lift to \mathbb{C}^3 is

$$(2-10) \quad \mathbf{q} = \mathbf{q}(\alpha, \beta, w) = \begin{bmatrix} -\frac{1}{2}r^2 e^{-i\alpha} \\ rwe^{i(-\alpha/2+\beta)} \\ 1 \end{bmatrix},$$

where $\alpha \in [-\frac{\pi}{2}, \frac{\pi}{2}]$, $\beta \in [0, \pi)$ and $w \in [-\sqrt{\cos(\alpha)}, \sqrt{\cos(\alpha)}]$. The ideal boundary of $S_{[0,0]}(r)$ on $\partial\mathbb{H}_{\mathbb{C}}^2$ consists of the points with $w = \pm\sqrt{\cos(\alpha)}$.

We are interested in the intersection of Cygan spheres.

Proposition 2.11 [22, Proposition 2.10] *The intersection of two Cygan spheres is connected.*

Remark 2.12 This intersection is often called a *Giraud disk*.

The following property should be useful to describe the intersection of Cygan spheres; see Proposition 2.12 of [22] or Example 5.1.8 of [12].

Proposition 2.13 *Let $S_{[0,0]}(r)$ be a Cygan sphere with geographical coordinates (α, β, w) .*

- (1) *The level sets of α are complex lines, called slices of $S_{[0,0]}(r)$.*
- (2) *The level sets of β are Lagrangian planes, called meridians of $S_{[0,0]}(r)$.*
- (3) *The set of points with $w = 0$ is the spine of $S_{[0,0]}(r)$. It is a geodesic contained in every meridian.*

A central part of this paper is constructing a polyhedron for a finitely generated subgroup of $\text{PU}(2, 1)$.

Definition 2.14 Let G be a discrete subgroup of $\text{PU}(2, 1)$. The *Ford polyhedron* D_G for G is the set

$$D_G = \{p \in \mathbb{H}_{\mathbb{C}}^2 \cup \partial\mathbb{H}_{\mathbb{C}}^2 : |\langle p, q_{\infty} \rangle| \leq |\langle p, g^{-1}q_{\infty} \rangle| \text{ for all } g \in G \text{ with } g(q_{\infty}) \neq q_{\infty}\}.$$

That is to say D_G is the intersection of closures of the exteriors of all the isometric spheres for elements of G which do not fix q_{∞} . In fact, the Ford polyhedron is the limit of Dirichlet polyhedra as the center point goes to q_{∞} .

3 The parameter space of complex hyperbolic (4, 4, ∞) triangle groups

In this section, we give a parameter space of the complex hyperbolic (4, 4, ∞) triangle groups.

Let $\theta \in [0, \frac{\pi}{2})$. Let I_1, I_2 and I_3 be the complex involutions on the complex lines C_1, C_2 and C_3 in complex hyperbolic space $\mathbb{H}_{\mathbb{C}}^2$ with polar vectors $\mathbf{n}_1, \mathbf{n}_2$ and \mathbf{n}_3 , respectively. By conjugating elements in $\text{PU}(2, 1)$, one can normalize so that $\partial C_3 = \{[z, 0] \in \mathcal{N} : |z| = \sqrt{2}\}$, $\partial C_1 = \{[z_1, t] \in \mathcal{N} : t \in \mathbb{R}\}$ and $\partial C_2 = \{[z_2, t] \in \mathcal{N} : t \in \mathbb{R}\}$. That is, ∂C_3 is the circle in the z -plane of the Heisenberg group with center the origin and radius $\sqrt{2}$, and ∂C_1 (resp. ∂C_2) is the vertical line whose projection on the z -plane of the Heisenberg group is the point z_1 (resp. z_2). Thus the polar vectors of the complex lines can be written as

$$\mathbf{n}_1 = \begin{bmatrix} z_1 \\ 1 \\ 0 \end{bmatrix}, \quad \mathbf{n}_2 = \begin{bmatrix} z_2 \\ 1 \\ 0 \end{bmatrix} \quad \text{and} \quad \mathbf{n}_3 = \begin{bmatrix} 1 \\ 0 \\ 1 \end{bmatrix}.$$

Since $\text{tr}(I_1 I_3) = \text{tr}(I_2 I_3) = 1$, we have $|z_1| = |z_2| = 1$. Then, up to rotation about the t -axis of the Heisenberg group, the \mathbb{C} -circles ∂C_1 and ∂C_2 can be normalized to be the sets $\partial C_1 = \{[-e^{-i\theta}, t] \in \mathcal{N} : t \in \mathbb{R}\}$ and $\partial C_2 = \{[e^{i\theta}, t] \in \mathcal{N} : t \in \mathbb{R}\}$.

Note that the \mathbb{C} -circles ∂C_1 and ∂C_2 coincide with each other if $\theta = \frac{\pi}{2}$. According to (2-4), the complex involutions I_1, I_2 and I_3 on the complex lines are given as

$$I_1 = \begin{bmatrix} -1 & 2e^{i\theta} & 2 \\ 0 & 1 & 2e^{-i\theta} \\ 0 & 0 & -1 \end{bmatrix}, \quad I_2 = \begin{bmatrix} -1 & -2e^{-i\theta} & 2 \\ 0 & 1 & -2e^{i\theta} \\ 0 & 0 & -1 \end{bmatrix}, \quad I_3 = \begin{bmatrix} 0 & 0 & 1 \\ 0 & -1 & 0 \\ 1 & 0 & 0 \end{bmatrix}.$$

Proposition 3.1 *Let $\theta \in [0, \frac{\pi}{2})$, and I_1, I_2 and I_3 be defined as above. Then $\langle I_1, I_2, I_3 \rangle$ is a complex hyperbolic (4, 4, ∞) triangle group. Furthermore, the element $I_1 I_3 I_2 I_3$ is nonelliptic if and only if $0 \leq \theta \leq \frac{\pi}{3}$.*

Proof By computing the products of two involutions

$$I_2 I_3 = \begin{bmatrix} 2 & 2e^{-i\theta} & -1 \\ -2e^{i\theta} & -1 & 0 \\ -1 & 0 & 0 \end{bmatrix}, \quad I_3 I_1 = \begin{bmatrix} 0 & 0 & -1 \\ 0 & -1 & -2e^{-i\theta} \\ -1 & e^{i\theta} & 2 \end{bmatrix},$$

and

$$I_2 I_1 = \begin{bmatrix} 1 & -4 \cos(\theta) & -4(1 + e^{-2i\theta}) \\ 0 & 1 & 4 \cos(\theta) \\ 0 & 0 & 1 \end{bmatrix}.$$

It is easy to verify that $I_2 I_3$ and $I_3 I_1$ are elliptic of order 4 and $I_2 I_1$ is unipotent. Thus $\langle I_1, I_2, I_3 \rangle$ is a complex hyperbolic $(4, 4, \infty)$ triangle group.

Since the trace of $I_1 I_3 I_2 I_3$ is $\text{tr}(I_1 I_3 I_2 I_3) = 7 + 8 \cos(2\theta)$, the element $I_1 I_3 I_2 I_3$ is elliptic if and only if

$$-1 \leq \text{tr}(I_1 I_3 I_2 I_3) = 7 + 8 \cos(2\theta) < 32,$$

that is, $\frac{\pi}{3} < \theta \leq \frac{\pi}{2}$. Thus $I_1 I_3 I_2 I_3$ is nonelliptic if and only if $0 \leq \theta \leq \frac{\pi}{3}$. Moreover, when $\theta = \frac{\pi}{3}$, the element $I_1 I_3 I_2 I_3$ is parabolic. \square

If $\theta = 0$, all entries of I_1, I_2 and I_3 are in the ring of integers \mathbb{Z} , and if $\theta = \frac{\pi}{3}$ all entries of I_1, I_2 and I_3 are in the ring of Eisenstein integers $\mathbb{Z}[-1 + i\frac{\sqrt{3}}{2}]$. In both cases, the group $\langle I_1, I_2, I_3 \rangle$ is arithmetic. Thus, we have the following proposition:

Proposition 3.2 (1) *If $\theta = 0$, then the group $\langle I_1, I_2, I_3 \rangle$ is discrete and preserves a Lagrangian plane.*

(2) *If $\theta = \frac{\pi}{3}$, then the group $\langle I_1, I_2, I_3 \rangle$ is discrete.*

4 The Ford domain

For $\theta \in [0, \frac{\pi}{3}]$, let $S = I_2 I_3$ and $T = I_2 I_1$. Then $\Gamma = \langle S, T \rangle$ is a subgroup of $\langle I_1, I_2, I_3 \rangle$ of index two. In this section, we will mainly prove that Γ is discrete. Our method is to construct a candidate Ford domain D (see Definition 4.12), then apply the Poincaré polyhedron theorem to show that D is a fundamental domain for the cosets of $\langle T \rangle$ in Γ , and also that Γ is discrete.

4.1 The isometric spheres

Definition 4.1 For $k \in \mathbb{Z}$, let

- \mathcal{I}_k^+ be the isometric sphere $\mathcal{I}(T^k S T^{-k}) = T^k \mathcal{I}(S)$ and c_k^+ be its center,
- \mathcal{I}_k^- be the isometric sphere $\mathcal{I}(T^k S^{-1} T^{-k}) = T^k \mathcal{I}(S^{-1})$ and c_k^- be its center,
- \mathcal{I}_k^* be the isometric sphere $\mathcal{I}(T^k S^2 T^{-k}) = T^k \mathcal{I}(S^2)$ and c_k^* be its center,

- \mathcal{I}_k^\diamond be the isometric sphere $\mathcal{I}(T^k(S^{-1}T)^2T^{-k}) = T^k\mathcal{I}((S^{-1}T)^2)$ and c_k^\diamond be its center.

Note that S and $S^{-1}T$ both have order 4, so $S^2 = S^{-2}$ and $(S^{-1}T)^2 = (S^{-1}T)^{-2}$. The centers and radii of the isometric spheres \mathcal{I}_k^+ , \mathcal{I}_k^- , \mathcal{I}_k^\star and \mathcal{I}_k^\diamond are listed in the following table:

isometric sphere	center	radius
\mathcal{I}_k^+	$c_k^+ = [4k \cos(\theta), 8k \sin(2\theta)]$	$\sqrt{2}$
\mathcal{I}_k^-	$c_k^- = [4k \cos(\theta) + 2e^{i\theta}, 0]$	$\sqrt{2}$
\mathcal{I}_k^\star	$c_k^\star = [4k \cos(\theta) + e^{i\theta}, 4k \sin(2\theta)]$	1
\mathcal{I}_k^\diamond	$c_k^\diamond = [4k \cos(\theta) - e^{-i\theta}, 4k \sin(2\theta)]$	1

Proposition 4.2 Let $k \in \mathbb{Z}$.

- (1) There is an antiholomorphic involution τ such that $\tau(\mathcal{I}_k^+) = \mathcal{I}_{-k}^+$, $\tau(\mathcal{I}_k^-) = \mathcal{I}_{-k-1}^-$ and $\tau(\mathcal{I}_k^\star) = \mathcal{I}_{-k}^\diamond$.
- (2) The complex involution I_2 interchanges \mathcal{I}_k^\star and \mathcal{I}_{-k}^\star , interchanges \mathcal{I}_k^+ and \mathcal{I}_{-k}^- , and interchanges \mathcal{I}_k^\diamond and $\mathcal{I}_{-k+1}^\diamond$.

Proof (1) Let $\tau: \mathbb{C}^3 \rightarrow \mathbb{C}^3$ be given by

$$\tau: \begin{bmatrix} z_1 \\ z_2 \\ z_3 \end{bmatrix} \mapsto \begin{bmatrix} \bar{z}_1 \\ -\bar{z}_2 \\ \bar{z}_3 \end{bmatrix}.$$

Then τ^2 is the identity. It is easy to see that τ fixes the polar vector \mathbf{n}_3 , and interchanges the polar vectors \mathbf{n}_1 and \mathbf{n}_2 . Thus τ conjugates I_3 to itself, I_1 to I_2 and vice versa. So τ conjugates T to T^{-1} , S to $T^{-1}S$, S^{-1} to $S^{-1}T$ and S^2 to $(T^{-1}S)^2 = (S^{-1}T)^2$. This implies that $\tau(\mathcal{I}_k^+) = \mathcal{I}_{-k}^+$, $\tau(\mathcal{I}_k^-) = \mathcal{I}_{-k-1}^-$ and $\tau(\mathcal{I}_k^\star) = \mathcal{I}_{-k}^\diamond$.

- (2) The statement is easily obtained by the facts $I_2SI_2 = S^{-1}$ and $I_2TI_2 = T^{-1}$. \square

Before we consider the intersections of two isometric spheres, we would like to give a useful technical lemma. Suppose that $q \in \mathcal{I}_0^+$. Then by (2-10) the lift of $q = q(\alpha, \beta, w)$ is given by

$$(4-1) \quad \mathbf{q} = \mathbf{q}(\alpha, \beta, w) = \begin{bmatrix} -e^{-i\alpha} \\ \sqrt{2}we^{i(-\alpha/2+\beta)} \\ 1 \end{bmatrix},$$

where $\alpha \in [-\frac{\pi}{2}, \frac{\pi}{2}]$, $\beta \in [0, \pi)$ and $w \in [-\sqrt{\cos(\alpha)}, \sqrt{\cos(\alpha)}]$.

Definition 4.3 Let (α, β, w) be the geographical coordinates of \mathcal{I}_0^+ . We define

$$\begin{aligned} f_0^*(\alpha, \beta, w) &= 2w^2 + 1 + \cos(\alpha) - \sqrt{2}w \cos(-\frac{1}{2}\alpha + \beta - \theta) - 2\sqrt{2}w \cos(\frac{1}{2}\alpha + \beta - \theta), \\ f_0^-(\alpha, \beta, w) &= 2w^2 + 1 + \cos(\alpha) - \sqrt{2}w \cos(\frac{1}{2}\alpha + \beta - \theta) - 2\sqrt{2}w \cos(-\frac{1}{2}\alpha + \beta - \theta), \\ f_{-1}^-(\alpha, \beta, w) &= 2w^2 + 1 + \cos(\alpha) + \sqrt{2}w \cos(\frac{1}{2}\alpha + \beta + \theta) + 2\sqrt{2}w \cos(-\frac{1}{2}\alpha + \beta + \theta). \end{aligned}$$

Lemma 4.4 Suppose that $\theta \in [0, \frac{\pi}{3}]$. Let $f_0^*(\alpha, \beta, w)$, $f_0^-(\alpha, \beta, w)$ and $f_{-1}^-(\alpha, \beta, w)$ be the functions in Definition 4.3. Suppose that $q \in \mathcal{I}_0^+$. Then

- (1) q lies on \mathcal{I}_0^* (resp. in its interior or exterior) if and only if $f_0^*(\alpha, \beta, w) = 0$ (resp. is negative or positive),
- (2) q lies on \mathcal{I}_0^- (resp. in its interior or exterior) if and only if $f_0^-(\alpha, \beta, w) = 0$ (resp. is negative or positive),
- (3) q lies on \mathcal{I}_{-1}^- (resp. in its interior or exterior) if and only if $f_{-1}^-(\alpha, \beta, w) = 0$ (resp. is negative or positive).

Proof (1) Any point $q \in \mathcal{I}_0^+$ lies on \mathcal{I}_0^* (resp. in its interior or exterior) if and only if the Cygan distance between q and the center of \mathcal{I}_0^* is 1 (resp. less than 1 or greater than 1). Using (4-1), the difference between the Cygan distance from q to the center of \mathcal{I}_0^* and 1 is

$$\begin{aligned} d_{\text{Cyg}}(q, c_0^*)^4 - 1 &= 4|-e^{-i\alpha} + \sqrt{2}we^{i(-\alpha/2 + \beta - \theta)} - \frac{1}{2}|^2 - 1 \\ &= 4(2w^2 + 1 + \cos(\alpha) - \sqrt{2}w \cos(-\frac{1}{2}\alpha + \beta - \theta) - 2\sqrt{2}w \cos(\frac{1}{2}\alpha + \beta - \theta)) \\ &= 4f_0^*(\alpha, \beta, w). \end{aligned}$$

Hence, q lies on \mathcal{I}_0^* (resp. in its interior or exterior) if and only if $f_0^*(\alpha, \beta, w) = 0$ (resp. negative or positive).

The rest of the proof runs as before. □

4.2 The intersection of isometric spheres

Proposition 4.5 Suppose that $\theta \in [0, \frac{\pi}{3}]$. Then each pair of isometric spheres in $\{\mathcal{I}_k^+ : k \in \mathbb{Z}\}$ is disjoint in $\mathbb{H}_{\mathbb{C}}^2 \cup \partial\mathbb{H}_{\mathbb{C}}^2$.

Proof It suffices to show that \mathcal{I}_0^+ and \mathcal{I}_k^+ are disjoint for $|k| \geq 1$. Observe that T is a Heisenberg translation associated with $[4 \cos(\theta), 8 \sin(2\theta)]$. According to the Cygan metric given in (2-2), the Cygan distance between the centers of \mathcal{I}_0^+ and \mathcal{I}_k^+ is

$$4\sqrt{|k| \cos(\theta)} \cdot |k \cos(\theta) - i \sin(\theta)|^{1/2} \geq 4\sqrt{\cos(\theta)} \geq 2\sqrt{2}.$$

Thus the Cygan distance between the centers of \mathcal{I}_0^+ and \mathcal{I}_k^+ is bigger than the sum of the radii, except when $k = \pm 1$ and $\theta = \frac{\pi}{3}$. This implies that \mathcal{I}_0^+ and \mathcal{I}_k^+ are disjoint for all $|k| \geq 2$.

When $k = \pm 1$ and $\theta = \frac{\pi}{3}$, although the Cygan distance between the centers of \mathcal{I}_0^+ and $\mathcal{I}_{\pm 1}^+$ is the sum of the radii, we claim that they are still disjoint. Using the symmetry τ in Proposition 4.2, we only need to show that $\mathcal{I}_0^+ \cap \mathcal{I}_1^+ = \emptyset$. Suppose that $q \in \mathcal{I}_0^+$. Using the geographical coordinates of $q = q(\alpha, \beta, w)$ given in (4-1), we can compute the difference between the Cygan distance of q and the center of \mathcal{I}_1^+ with its radius. That is,

$$\begin{aligned} d_{\text{Cyg}}(q, [2, 4\sqrt{3}])^4 - 4 &= 4|-e^{-i\alpha} + \sqrt{2}we^{i(-\alpha/2+\beta-\theta)} - 4e^{i\pi/3}|^2 - 4 \\ &= 32\left(w^2 + \frac{\sqrt{2}}{2}w(\cos(\frac{1}{2}\alpha + \beta) + 2\cos(\frac{1}{2}\alpha - \beta + \frac{\pi}{3})) + \cos(\alpha + \frac{\pi}{3}) + 2\right) \\ &= 32f(\alpha, \beta, w). \end{aligned}$$

Here $f(\alpha, \beta, w)$ can be seen as a quadratic function of w . Let

$$B = \frac{\sqrt{2}}{2}(\cos(\frac{1}{2}\alpha + \beta) + 2\cos(\frac{1}{2}\alpha - \beta + \frac{\pi}{3}))$$

and $C = \cos(\alpha + \frac{\pi}{3}) + 2$. If $B^2 - 4C < 0$, then it is obvious that $f(\alpha, \beta, w) > 0$. If $B^2 - 4C \geq 0$, then $B \leq -2\sqrt{C}$ (which is impossible by numerical computation) or $B \geq 2\sqrt{C}$. In this case we have $B - 2\sqrt{\cos(\alpha)} \geq B - 2\sqrt{C} \geq 0$ since $\cos(\alpha) \leq C$. This means that the symmetry axes of f lie on the left side of $w = -\sqrt{\cos(\alpha)}$. Besides, one can compute numerically that $f(\alpha, \beta, -\sqrt{\cos(\alpha)}) > 0$ on the range of α and β . So, we have $f(\alpha, \beta, w) > 0$. This means that every point on \mathcal{I}_0^+ lies outside of \mathcal{I}_1^+ . Hence $\mathcal{I}_0^+ \cap \mathcal{I}_1^+ = \emptyset$. □

By a similar argument, we have the following propositions:

Proposition 4.6 *Suppose that $\theta \in [0, \frac{\pi}{3}]$. Then*

- (1) \mathcal{I}_0^+ and \mathcal{I}_k^- are disjoint in $\mathbb{H}_{\mathbb{C}}^2 \cup \partial\mathbb{H}_{\mathbb{C}}^2$, except possibly when $k = -1, 0$,
- (2) \mathcal{I}_0^+ and \mathcal{I}_k^* are disjoint in $\mathbb{H}_{\mathbb{C}}^2 \cup \partial\mathbb{H}_{\mathbb{C}}^2$, except possibly when $k = -1, 0$,
- (3) \mathcal{I}_0^+ and \mathcal{I}_k^{\otimes} are disjoint in $\mathbb{H}_{\mathbb{C}}^2 \cup \partial\mathbb{H}_{\mathbb{C}}^2$, except possibly when $k = 0, 1$.

Proposition 4.7 *Suppose that $\theta \in [0, \frac{\pi}{3}]$. Then:*

- (1) \mathcal{I}_0^\star and \mathcal{I}_k^\star are disjoint in $\mathbb{H}_\mathbb{C}^2$. Furthermore, when $\theta = \frac{\pi}{3}$ the closures of \mathcal{I}_0^\star and \mathcal{I}_{-1}^\star (respectively, \mathcal{I}_1^\star) are tangent at the parabolic fixed point of $T^{-1}S^2$ (respectively, $T(T^{-1}S^2)T^{-1}$) on $\partial\mathbb{H}_\mathbb{C}^2$.
- (2) \mathcal{I}_0^\star and \mathcal{I}_k^\diamond are disjoint in $\mathbb{H}_\mathbb{C}^2 \cup \partial\mathbb{H}_\mathbb{C}^2$, except possibly when $k = 0, 1$.

Lemma 4.8 Suppose that $\theta \in [0, \frac{\pi}{3}]$. Then $\mathcal{I}_0^+ \cap \mathcal{I}_0^\star \cap \mathcal{I}_{-1}^- = \emptyset$ except when $\theta = \frac{\pi}{3}$, in which case the triple intersection is the point $[e^{i2\pi/3}, -\sqrt{3}] \in \partial\mathbb{H}_\mathbb{C}^2$. Moreover, this point is the parabolic fixed point of $T^{-1}S^2$.

Proof Suppose that $q \in \mathcal{I}_0^+$. Using Lemma 4.4, the geographical coordinates (α, β, w) of $q \in \mathcal{I}_0^+ \cap \mathcal{I}_0^\star \cap \mathcal{I}_{-1}^-$ should satisfy

$$(4-2) \quad 2w^2 + 1 + \cos(\alpha) - \sqrt{2}w \cos(-\frac{1}{2}\alpha + \beta - \theta) - 2\sqrt{2}w \cos(\frac{1}{2}\alpha + \beta - \theta) = 0,$$

$$(4-3) \quad 2w^2 + 1 + \cos(\alpha) + \sqrt{2}w \cos(\frac{1}{2}\alpha + \beta + \theta) + 2\sqrt{2}w \cos(-\frac{1}{2}\alpha + \beta + \theta) = 0.$$

Subtracting (4-2) and (4-3),

$$2\sqrt{2}w \cos(\beta) (\cos(\frac{1}{2}\alpha + \theta) + 2 \cos(\frac{1}{2}\alpha - \theta)) = 0.$$

This implies that either $w = 0$ or $\beta = \frac{\pi}{2}$, since $(\cos(\frac{1}{2}\alpha + \theta) + 2 \cos(\frac{1}{2}\alpha - \theta)) \neq 0$ for $\theta \in [0, \frac{\pi}{3}]$. We know that the points with $w = 0$ lie in the meridian with $\beta = \frac{\pi}{2}$. Therefore, a necessary condition for $q \in \mathcal{I}_0^+ \cap \mathcal{I}_0^\star \cap \mathcal{I}_{-1}^-$ is that $\beta = \frac{\pi}{2}$.

Substituting $\beta = \frac{\pi}{2}$ into (4-2) and simplifying,

$$(4-4) \quad 2w^2 + 2 \cos^2(\frac{1}{2}\alpha) + \sqrt{2}w (\sin(\frac{1}{2}\alpha) \cos(\theta) - 3 \cos(\frac{1}{2}\alpha) \sin(\theta)) = 0.$$

Let $b(\alpha, \theta) = \sin(\frac{1}{2}\alpha) \cos(\theta) - 3 \cos(\frac{1}{2}\alpha) \sin(\theta)$. It is easy to see that, for every α , the function $\theta \mapsto b(\alpha, \theta)$ is decreasing on $[0, \frac{\pi}{3}]$.

The left-hand side of (4-4) can be seen as a quadratic function of w with positive leading coefficient. Thus (4-4) has at least one solution only if $b^2 - 8 \cos^2(\frac{1}{2}\alpha) \geq 0$, that is $b \geq 2\sqrt{2} \cos(\frac{1}{2}\alpha)$, which is impossible since $b \leq b(\alpha, 0) = \sin(\frac{1}{2}\alpha)$, or $b \leq -2\sqrt{2} \cos(\frac{1}{2}\alpha)$. Since $\sqrt{\cos(\alpha)} \leq \cos(\frac{1}{2}\alpha)$, we have $b + 2\sqrt{2} \sqrt{\cos(\alpha)} \leq b + 2\sqrt{2} \cos(\frac{1}{2}\alpha) \leq 0$. This means that the symmetry axes of the quadratic function lie on the right-hand side of $w = \sqrt{\cos(\alpha)}$.

Besides, one can compute that

$$\begin{aligned} & b\sqrt{\cos(\alpha)} + \sqrt{2}(\cos(\alpha) + \cos^2(\frac{1}{2}\alpha)) \\ & \geq (\sin(\frac{1}{2}\alpha) \cos(\frac{\pi}{3}) - 3 \cos(\frac{1}{2}\alpha) \sin(\frac{\pi}{3}))\sqrt{\cos(\alpha)} + \sqrt{2}(\cos(\alpha) + \cos^2(\frac{1}{2}\alpha)) \\ & = \frac{\sqrt{2}}{2} (\frac{1}{2} \sqrt{\cos(\alpha)} + \frac{\sqrt{2}}{2} \sin(\frac{1}{2}\alpha))^2 + \frac{3\sqrt{2}}{2} (\frac{\sqrt{3}}{2} \sqrt{\cos(\alpha)} - \frac{\sqrt{2}}{2} \cos(\frac{1}{2}\alpha))^2. \end{aligned}$$

Then $b\sqrt{\cos(\alpha)} + \sqrt{2}(\cos(\alpha) + \cos^2(\frac{1}{2}\alpha)) \geq 0$. If it is 0, then $\alpha = -\frac{\pi}{3}$ and $\theta = \frac{\pi}{3}$. This means that for $w \in [-\sqrt{\cos(\alpha)}, \sqrt{\cos(\alpha)}]$ equation (4-4) has no solution except when $\theta = \frac{\pi}{3}$ and $\alpha = -\frac{\pi}{3}$, in which case $w = \sqrt{\cos(\alpha)} = \frac{\sqrt{2}}{2}$.

Hence $q \in \mathcal{I}_0^+ \cap \mathcal{I}_0^* \cap \mathcal{I}_{-1}^-$ if and only if $\theta = \frac{\pi}{3}$, $\alpha = -\frac{\pi}{3}$ and $w = \sqrt{\cos(\alpha)} = \frac{\sqrt{2}}{2}$. When $\theta = \frac{\pi}{3}$, $T^{-1}S^2$ is unipotent and its fixed point is the eigenvector with eigenvalue 1. One can compute that its fixed point is $[e^{i2\pi/3}, -\sqrt{3}] \in \partial\mathbb{H}_{\mathbb{C}}^2$, which equals the point $q(-\frac{\pi}{3}, \frac{\pi}{2}, \frac{\sqrt{2}}{2})$. □

Proposition 4.9 *Suppose that $\theta \in [0, \frac{\pi}{3}]$. Then:*

- (1) *The intersection $\mathcal{I}_0^* \cap \mathcal{I}_0^\diamond$ lies in the interior of \mathcal{I}_0^+ .*
- (2) *The intersection $\mathcal{I}_0^* \cap \mathcal{I}_{-1}^-$ either is empty or lies in the interior of \mathcal{I}_0^+ . Further, when $\theta = \frac{\pi}{3}$, there is a unique point on the ideal boundary of $\mathcal{I}_0^* \cap \mathcal{I}_{-1}^-$ on $\partial\mathbb{H}_{\mathbb{C}}^2$, which is fixed by $T^{-1}S^2$, lying on the ideal boundary of \mathcal{I}_0^+ .*

Proof (1) Let $p = (z, t, u) \in \mathcal{I}_0^* \cap \mathcal{I}_0^\diamond$, then p satisfies the equations

$$||z - e^{i\theta}|^2 + u - i(t + 2\text{Im}(ze^{-i\theta}))| = 1, \quad ||z + e^{-i\theta}|^2 + u - i(t + 2\text{Im}(-ze^{i\theta}))| = 1.$$

Set $z = |z|e^{i\phi}$. By simplifying, we have

$$||z|^2 + 1 + u - 2|z| \cos(\phi - \theta) - i(t + 2|z| \sin(\phi - \theta))| = 1,$$

$$||z|^2 + 1 + u + 2|z| \cos(\phi + \theta) - i(t - 2|z| \sin(\phi + \theta))| = 1.$$

Now set

$$(4-5) \quad |z|^2 + 1 + u - 2|z| \cos(\phi - \theta) - i(t + 2|z| \sin(\phi - \theta)) = e^{i\alpha},$$

$$(4-6) \quad |z|^2 + 1 + u + 2|z| \cos(\phi + \theta) - i(t - 2|z| \sin(\phi + \theta)) = e^{i\beta}.$$

Since

$$\cos \alpha = |z|^2 + 1 + u - 2|z| \cos(\phi - \theta) = (|z| - \cos(\phi - \theta))^2 + \sin^2(\phi - \theta) + u \geq 0$$

and

$$\cos \beta = |z|^2 + 1 + u + 2|z| \cos(\phi + \theta) = (|z| + \cos(\phi + \theta))^2 + \sin^2(\phi + \theta) + u \geq 0,$$

we have $-\frac{\pi}{2} \leq \alpha \leq \frac{\pi}{2}$ and $-\frac{\pi}{2} \leq \beta \leq \frac{\pi}{2}$. Thus $\cos(\frac{1}{2}\beta - \frac{1}{2}\alpha) \geq 0$. By computing the difference of (4-5) and (4-6), we have

$$(4-7) \quad z = \frac{e^{i\beta} - e^{i\alpha}}{4 \cos(\theta)} = \pm \frac{\sin(\frac{1}{2}\beta - \frac{1}{2}\alpha)}{2 \cos(\theta)} e^{i(\pm\pi/2 + \beta/2 + \alpha/2)}.$$

Thus $\phi = \pm \frac{\pi}{2} + \frac{1}{2}\beta + \frac{1}{2}\alpha$. Therefore,

$$\begin{aligned} & (|z|^2 + u)^2 + t^2 \\ &= (\cos(\alpha) - 1 + 2|z| \cos(\phi - \theta))^2 + (\sin(\alpha) + 2|z| \sin(\phi - \theta))^2 \\ &= 2 + 4|z|^2 - 2 \cos(\alpha) - 4|z| \cos(\phi - \theta) + 4|z| \cos(\phi - \theta - \alpha) \\ &\leq 2 + 4|z|^2 - 2(|z|^2 + 1 - 2|z| \cos(\phi - \theta)) - 4|z| \cos(\phi - \theta) + 4|z| \cos(\phi - \theta - \alpha) \\ &= 2|z|^2 + 4|z| \cos(\phi - \theta - \alpha) = 2|z|^2 + 4|z| \cos(\pm \frac{\pi}{2} - \theta + \frac{1}{2}\beta - \frac{1}{2}\alpha) \\ &= 2|z|^2 + 4|z|(\pm \sin(\theta) \cos(\frac{1}{2}\beta - \frac{1}{2}\alpha) \mp \cos(\theta) \sin(\frac{1}{2}\beta - \frac{1}{2}\alpha)) \\ &= \frac{\sin^2(\frac{1}{2}\beta - \frac{1}{2}\alpha)}{2 \cos^2(\theta)} + \tan(\theta) \sin(\beta - \alpha) - 2 \sin^2(\frac{1}{2}\beta - \frac{1}{2}\alpha). \end{aligned}$$

Since $\theta \in [0, \frac{\pi}{3}]$, we have that $\sin^2(\frac{1}{2}\beta - \frac{1}{2}\alpha)/(2 \cos^2(\theta)) \leq 2 \sin^2(\frac{1}{2}\beta - \frac{1}{2}\alpha)$ and $\tan(\theta) \sin(\beta - \alpha) \leq \sqrt{3}$. This implies that $(|z|^2 + u)^2 + t^2 < 4$, so the intersection $\mathcal{I}_0^* \cap \mathcal{I}_0^\circ$ lies in the interior of \mathcal{I}_0^+ .

(2) Suppose that $p = (z, t, u) \in \mathcal{I}_0^* \cap \mathcal{I}_1^-$. Then p satisfies the equations

$$\begin{aligned} 1 &= \left| |z - e^{i\theta}|^2 + u - i(t + 2 \operatorname{Im}(ze^{-i\theta})) \right| = \left| |z|^2 + u + 1 - it - 2ze^{-i\theta} \right|, \\ 2 &= \left| |z + 2e^{-i\theta}|^2 + u - i(t + 2 \operatorname{Im}(-2ze^{i\theta})) \right| = \left| |z|^2 + u + 4 - it + 4ze^{i\theta} \right|. \end{aligned}$$

Now set

$$(4-8) \quad |z|^2 + u + 1 - it - 2ze^{-i\theta} = e^{i\beta},$$

$$(4-9) \quad |z|^2 + u + 4 - it + 4ze^{i\theta} = 2e^{i\alpha}.$$

By computing the difference of (4-8) and (4-9), we have

$$(4-10) \quad z = \frac{2e^{i\alpha} - e^{i\beta} - 3}{4e^{i\theta} + 2e^{-i\theta}}.$$

According to (4-8),

$$(4-11) \quad u = \cos(\beta) - |ze^{-i\theta} - 1|^2,$$

$$(4-12) \quad t = -\sin(\beta) - 2 \operatorname{Im}(ze^{-i\theta}).$$

Since

$$\cos \beta = u + |ze^{-i\theta} - 1|^2 \geq 0 \quad \text{and} \quad 2 \cos \alpha = u + |ze^{i\theta} + 2|^2 \geq 0,$$

we have $-\frac{\pi}{2} \leq \alpha \leq \frac{\pi}{2}$ and $-\frac{\pi}{2} \leq \beta \leq \frac{\pi}{2}$.

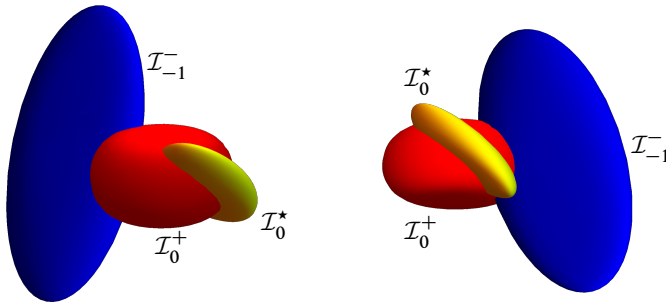


Figure 1: The ideal boundaries of the three spheres \mathcal{I}_0^+ , \mathcal{I}_{-1}^- and \mathcal{I}_0^* on $\partial\mathbb{H}_{\mathbb{C}}^2$. (On the left is the case when $\theta = 0$ and on the right is $\theta = \frac{\pi}{3}$.)

Now let us consider the case when $\theta = \frac{\pi}{3}$. Substituting $\alpha = \frac{\pi}{6}$ and $\beta = 0$ into (4-10), (4-11) and (4-12), we obtain the point

$$p_0 = \left(\frac{1}{3}(-3 + \sqrt{3}) + i\frac{1}{6}(3 + \sqrt{3}), \frac{1}{6}(3 - 7\sqrt{3}), \frac{1}{6}(-13 + 8\sqrt{3})\right) \in \mathcal{I}_0^* \cap \mathcal{I}_{-1}^-.$$

One can compute that p_0 lies in the interior of \mathcal{I}_0^+ , since

$$||z|^2 + u - it|^2 = |e^{i\beta} - 1 + 2ze^{-i\theta}|^2 = 4|z|^2 = \frac{20}{3} - 2\sqrt{3} < 4.$$

We know that $\mathcal{I}_0^* \cap \mathcal{I}_{-1}^-$ is connected from Proposition 2.11. Thus, according to Lemma 4.8, $\mathcal{I}_0^* \cap \mathcal{I}_{-1}^-$ lies in the interior of \mathcal{I}_0^+ except the point $[e^{i2\pi/3}, -\sqrt{3}]$, which lies on the ideal boundary of \mathcal{I}_0^+ ; see Figure 1.

Observe that coordinates of the centers of \mathcal{I}_0^* and \mathcal{I}_{-1}^- are continuous on θ . Thus the geometric positions of the spheres \mathcal{I}_0^* and \mathcal{I}_{-1}^- depend continuously on θ . When $\theta = 0$, since the Cygan distance between the centers of \mathcal{I}_0^* and \mathcal{I}_{-1}^- is bigger than the sum of their radii, one can see that $\mathcal{I}_0^* \cap \mathcal{I}_{-1}^- = \emptyset$. When $\theta = \frac{\pi}{3}$, we have shown that $\mathcal{I}_0^* \cap \mathcal{I}_{-1}^-$ lies in the interior of \mathcal{I}_0^+ . We also have $\mathcal{I}_0^+ \cap \mathcal{I}_0^* \cap \mathcal{I}_{-1}^- = \emptyset$ for $\theta \in [0, \frac{\pi}{3})$ by Lemma 4.8. Hence, the intersection $\mathcal{I}_0^* \cap \mathcal{I}_{-1}^-$ is either empty or contained in the interior of \mathcal{I}_0^+ . □

Proposition 4.10 Suppose that $\theta \in [0, \frac{\pi}{3}]$. For $k \in \mathbb{Z}$, the three isometric spheres \mathcal{I}_k^+ , \mathcal{I}_k^- and \mathcal{I}_k^* (resp. \mathcal{I}_k^+ , \mathcal{I}_{k-1}^- and \mathcal{I}_k^\diamond) have the following properties:

- The intersections $\mathcal{I}_k^+ \cap \mathcal{I}_k^-$, $\mathcal{I}_k^- \cap \mathcal{I}_k^*$ and $\mathcal{I}_k^* \cap \mathcal{I}_k^+$ (resp. $\mathcal{I}_k^+ \cap \mathcal{I}_{k-1}^-$, $\mathcal{I}_{k-1}^- \cap \mathcal{I}_k^\diamond$ and $\mathcal{I}_k^\diamond \cap \mathcal{I}_k^+$) are discs.
- The intersection $\mathcal{I}_k^+ \cap \mathcal{I}_k^- \cap \mathcal{I}_k^*$ (resp. $\mathcal{I}_k^+ \cap \mathcal{I}_{k-1}^- \cap \mathcal{I}_k^\diamond$) is a union of two geodesics which are crossed at the fixed point of $T^k S T^{-k}$ (resp. $T^k(S^{-1}T)T^{-k}$) in $\mathbb{H}_{\mathbb{C}}^2$.

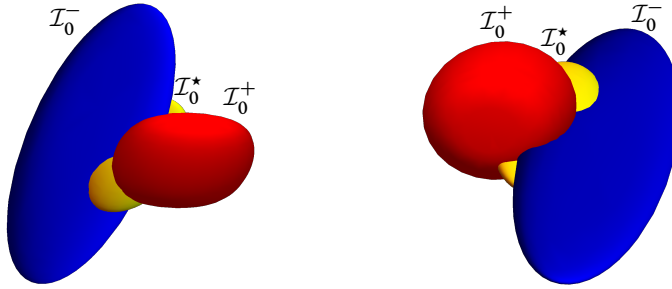


Figure 2: The ideal boundaries of the three spheres \mathcal{I}_0^+ , \mathcal{I}_0^- and \mathcal{I}_0^* on $\partial\mathbb{H}_{\mathbb{C}}^2$. (On the left is the case when $\theta = 0$ and on the right is $\theta = \frac{\pi}{3}$.)

and whose four endpoints are on $\partial\mathbb{H}_{\mathbb{C}}^2$. Moreover, the four rays from the fixed point to the four endpoints are cyclically permuted by $T^k ST^{-k}$ (resp. $T^k(S^{-1}T)T^{-k}$).

Proof According to Definition 4.1 and Proposition 4.2, it suffices to consider the isometric spheres \mathcal{I}_0^+ , \mathcal{I}_0^- and \mathcal{I}_0^* ; see Figure 2.

Let $q \in \mathcal{I}_0^+$. Consider the geographical coordinates (α, β, w) of q in (4-1). By Lemma 4.4, if q lies on $\mathcal{I}_0^+ \cap \mathcal{I}_0^-$, then α, β and w should satisfy the equation

$$(4-13) \quad 2w^2 + 1 + \cos(\alpha) - \sqrt{2}w \cos(\frac{1}{2}\alpha + \beta - \theta) - 2\sqrt{2}w \cos(-\frac{1}{2}\alpha + \beta - \theta) = 0.$$

Similarly, if q lies on $\mathcal{I}_0^+ \cap \mathcal{I}_0^*$, then α, β and w should satisfy the equation

$$(4-14) \quad 2w^2 + 1 + \cos(\alpha) - \sqrt{2}w \cos(-\frac{1}{2}\alpha + \beta - \theta) - 2\sqrt{2}w \cos(\frac{1}{2}\alpha + \beta - \theta) = 0.$$

Thus $\mathcal{I}_0^+ \cap \mathcal{I}_0^-$ is the set of solutions of (4-13) and $\mathcal{I}_0^+ \cap \mathcal{I}_0^*$ is the set of solutions of (4-14). One can easily verify that the geographical coordinates of the point $q(0, \theta, \frac{\sqrt{2}}{2}) \in \mathbb{H}_{\mathbb{C}}^2$ satisfy (4-13) and (4-14), so the intersections $\mathcal{I}_0^+ \cap \mathcal{I}_0^-$ and $\mathcal{I}_0^+ \cap \mathcal{I}_0^*$ are topological discs from Proposition 2.11.

The intersection of these two sets gives the triple intersection $\mathcal{I}_0^+ \cap \mathcal{I}_0^- \cap \mathcal{I}_0^*$. Now let us solve the system of equations (4-13) and (4-14). Let $t = \beta - \theta$. Subtracting (4-13) and (4-14) and simplifying, we obtain

$$2w \sin(\frac{1}{2}\alpha) \sin(t) = 0.$$

Thus $w = 0$ (this is impossible), $\alpha = 0$, or $t = 0$. If $t = 0$, then setting $\beta = \theta$ in (4-13), we get

$$2w^2 - 3\sqrt{2} \cos(\frac{1}{2}\alpha)w + 1 + \cos(\alpha) = 2(w - \frac{1}{2}\sqrt{2} \cos(\frac{1}{2}\alpha))(w - \sqrt{2} \cos(\frac{1}{2}\alpha)) = 0.$$

Note that the solutions of the above equation for w should satisfy $w^2 \leq \cos(\alpha)$. Thus

$$w = \frac{1}{2}\sqrt{2}\cos\left(\frac{1}{2}\alpha\right) \quad \text{with } \cos(\alpha) \geq \frac{1}{3}.$$

If $\alpha = 0$, then (4-13) becomes

$$(4-15) \quad 2w^2 - 3\sqrt{2}\cos(t)w + 2 = 0.$$

Note that the solutions of (4-15) for w should satisfy $w^2 \leq \cos(\alpha) = 1$. Thus the solutions of (4-15) are

$$w = \frac{3\cos(t) - \sqrt{9\cos^2(t) - 8}}{2\sqrt{2}} \quad \text{with } \frac{2\sqrt{2}}{3} \leq \cos(t) \leq 1,$$

and

$$w = \frac{3\cos(t) + \sqrt{9\cos^2(t) - 8}}{2\sqrt{2}} \quad \text{with } -1 \leq \cos(t) \leq -\frac{2\sqrt{2}}{3}.$$

So the triple intersection $\mathcal{I}_0^+ \cap \mathcal{I}_0^- \cap \mathcal{I}_0^*$ is the union $\mathcal{L}_1 \cup \mathcal{C}_1 \cup \mathcal{C}_2$, where

$$\mathcal{L}_1 = \{q(\alpha, t + \theta, w) \in \mathcal{I}_0^+ : \cos(\alpha) \geq \frac{1}{3}, t = 0 \text{ and } w = \frac{1}{2}\sqrt{2}\cos\left(\frac{1}{2}\alpha\right)\},$$

$$\mathcal{C}_1 = \left\{q(0, t + \theta, w) \in \mathcal{I}_0^+ : \frac{2\sqrt{2}}{3} \leq \cos(t) \leq 1 \text{ and } w = \frac{3\cos(t) - \sqrt{9\cos^2(t) - 8}}{2\sqrt{2}}\right\},$$

and

$$\mathcal{C}_2 = \left\{q(0, t + \theta, w) \in \mathcal{I}_0^+ : -1 \leq \cos(t) \leq -\frac{2\sqrt{2}}{3}, w = \frac{3\cos(t) + \sqrt{9\cos^2(t) - 8}}{2\sqrt{2}}\right\}.$$

Note that \mathcal{L}_1 lies in a Lagrangian plane of \mathcal{I}_0^+ , and $\mathcal{C}_1 \cup \mathcal{C}_2$ lies in a complex line of \mathcal{I}_0^+ . It is obvious that \mathcal{C}_1 is an arc. One of its endpoints is $q(0, \theta, \frac{\sqrt{2}}{2}) \in \mathbb{H}_{\mathbb{C}}^2$, which is the fixed point of S . The other one is $q(0, \arccos(\frac{2\sqrt{2}}{3}) + \theta, 1) \in \partial\mathbb{H}_{\mathbb{C}}^2$. Similarly, \mathcal{C}_2 is an arc with endpoints $q(0, \theta, \frac{\sqrt{2}}{2})$ and $q(0, \arccos(-\frac{2\sqrt{2}}{3}) + \theta, -1) \in \partial\mathbb{H}_{\mathbb{C}}^2$. Thus $\mathcal{C}_1 \cup \mathcal{C}_2$ is connected. The endpoints of \mathcal{L}_1 are $q(\arccos(\frac{1}{3}), \theta, \frac{\sqrt{3}}{3})$ and $q(-\arccos(\frac{1}{3}), \theta, \frac{\sqrt{3}}{3})$, which are on $\partial\mathbb{H}_{\mathbb{C}}^2$. It is easy to see that \mathcal{L}_1 intersects with $\mathcal{C}_1 \cup \mathcal{C}_2$ at the point $q(0, \theta, \frac{\sqrt{2}}{2}) \in \mathbb{H}_{\mathbb{C}}^2$.

Moreover, $\mathcal{C}_1 \cup \mathcal{C}_2$ is a geodesic. In fact, the complex line containing $\mathcal{C}_1 \cup \mathcal{C}_2$ is $\mathcal{C} = \{(-1, z) \in \mathbb{H}_{\mathbb{C}}^2 \cup \partial\mathbb{H}_{\mathbb{C}}^2 : |z| \leq \sqrt{2}\}$. This is a disc bounded by the circle with center the origin and radius $\sqrt{2}$, while $\mathcal{C}_1 \cup \mathcal{C}_2$ lies in the circle with center $\frac{3}{2}e^{i\theta}$ and radius $\frac{1}{2}$, which is orthogonal to the boundary of the complex line. The Cayley transform given in Definition 2.2 maps \mathcal{C} to the vertical axis $\{(0, z) \in \mathbb{H}_{\mathbb{C}}^2 \cup \partial\mathbb{H}_{\mathbb{C}}^2 : |z| \leq 1\}$ in the ball

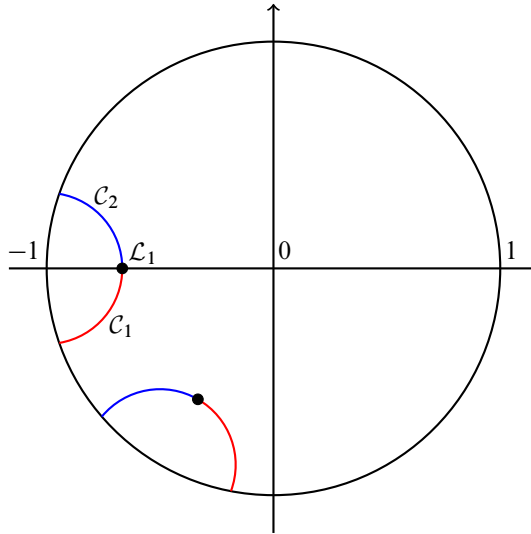


Figure 3: The triple intersection $\mathcal{I}_0^+ \cap \mathcal{I}_0^- \cap \mathcal{I}_0^*$ viewed on the vertical axis in the ball model of $\mathbb{H}_{\mathbb{C}}^2$. The blue curve is \mathcal{C}_1 and the red one is \mathcal{C}_2 . The black point on the curve is the projection of \mathcal{L}_1 on the complex line. The left curve is the case when $\theta = 0$ and the one on the lower left is the case when $\theta = \frac{\pi}{3}$.

model of $\mathbb{H}_{\mathbb{C}}^2$. Thus \mathcal{C} is isometric to the Poincaré disc. Then $\mathcal{C}_1 \cup \mathcal{C}_2$ is mapped by the Cayley transform to an arc contained in the circle with center $-3e^{i\theta}/(2\sqrt{2})$ and radius $1/(2\sqrt{2})$, which is orthogonal to the unit circle. Hence $\mathcal{C}_1 \cup \mathcal{C}_2$ is a geodesic; see Figure 3.

The Cayley transform maps \mathcal{L}_1 to $\{(-\tan(\frac{1}{2}\alpha)i, -e^{i\theta}/\sqrt{2}) \in \mathbb{H}_{\mathbb{C}}^2 \cup \partial\mathbb{H}_{\mathbb{C}}^2 : \cos(\alpha) \geq \frac{1}{3}\}$. Thus \mathcal{L}_1 and $\mathcal{C}_1 \cup \mathcal{C}_2$ are crossed at the point $(0, -e^{i\theta}/\sqrt{2}) \in \mathbb{H}_{\mathbb{C}}^2$, which is the image of $q(0, \theta, \frac{\sqrt{2}}{2})$ under the Cayley transform.

It is easy to check that $S(q(0, \theta, \frac{\sqrt{2}}{2})) = q(0, \theta, \frac{\sqrt{2}}{2})$, and that the other four points are cyclically permuted by S :

$$\begin{array}{ccc}
 q(0, \arccos(\frac{2\sqrt{2}}{3}) + \theta, 1) & \xrightarrow{S} & q(\arccos(\frac{1}{3}), \theta, \frac{\sqrt{3}}{3}) \\
 \uparrow S & & \downarrow S \\
 q(-\arccos(\frac{1}{3}), \theta, \frac{\sqrt{3}}{3}) & \xleftarrow{S} & q(0, \arccos(-\frac{2\sqrt{2}}{3}) + \theta, -1)
 \end{array}$$

Moreover, it is easy to verify that $\mathcal{C}_1 \cup \mathcal{C}_2 = S(\mathcal{L}_1)$, $S^2(\mathcal{L}_1) = \mathcal{L}_1$ and $S^2(\mathcal{C}_1) = \mathcal{C}_2$. Thus, the four rays from the fixed point to the four endpoints are cyclically permuted by S . \square

By applying powers of T and the symmetries in Proposition 4.2 to Propositions 4.6, 4.7 and 4.9, all pairwise intersections of the isometric spheres can be summarized:

Corollary 4.11 *Suppose that $\theta \in [0, \frac{\pi}{3}]$. Let $\mathcal{S} = \{\mathcal{I}_k^\pm, \mathcal{I}_k^*, \mathcal{I}_k^\diamond : k \in \mathbb{Z}\}$ be the set of all the isometric spheres. Then for all $k \in \mathbb{Z}$:*

- (1) \mathcal{I}_k^+ is contained in the exterior of all the isometric spheres in \mathcal{S} except $\mathcal{I}_k^-, \mathcal{I}_{k-1}^-, \mathcal{I}_k^*, \mathcal{I}_{k-1}^*, \mathcal{I}_k^\diamond$ and $\mathcal{I}_{k+1}^\diamond$. Moreover, $\mathcal{I}_k^+ \cap \mathcal{I}_{k-1}^*$ (resp. $\mathcal{I}_k^+ \cap \mathcal{I}_{k+1}^\diamond$) is either empty or contained in the interior of \mathcal{I}_{k-1}^- (resp. \mathcal{I}_k^-). When $\theta = \frac{\pi}{3}$, $\mathcal{I}_k^+ \cap \mathcal{I}_{k-1}^*$ (resp. $\mathcal{I}_k^+ \cap \mathcal{I}_{k+1}^\diamond$) will be tangent with \mathcal{I}_{k-1}^- (resp. \mathcal{I}_k^-) on $\partial\mathbb{H}_\mathbb{C}^2$ at the parabolic fixed point of $T^k(S^2T)T^{-k}$ (resp. $T^k(S^{-1}TS^{-1})T^{-k}$).
- (2) \mathcal{I}_k^- is contained in the exterior of all the isometric spheres in \mathcal{S} except $\mathcal{I}_k^+, \mathcal{I}_{k+1}^+, \mathcal{I}_k^*, \mathcal{I}_{k+1}^*, \mathcal{I}_k^\diamond$ and $\mathcal{I}_{k+1}^\diamond$. Moreover, $\mathcal{I}_k^- \cap \mathcal{I}_k^\diamond$ (resp. $\mathcal{I}_k^- \cap \mathcal{I}_{k+1}^*$) is either empty or contained in the interior of \mathcal{I}_k^+ (resp. \mathcal{I}_{k+1}^+). When $\theta = \frac{\pi}{3}$, $\mathcal{I}_k^- \cap \mathcal{I}_k^\diamond$ (resp. $\mathcal{I}_k^- \cap \mathcal{I}_{k+1}^*$) will be tangent with \mathcal{I}_k^+ (resp. \mathcal{I}_{k+1}^+) on $\partial\mathbb{H}_\mathbb{C}^2$ at the parabolic fixed point of $T^k(ST^{-1}S)T^{-k}$ (resp. $T^k(S^2T^{-1})T^{-k}$).
- (3) \mathcal{I}_k^* is contained in the exterior of all the isometric spheres in \mathcal{S} except $\mathcal{I}_k^\pm, \mathcal{I}_{k+1}^+, \mathcal{I}_{k-1}^-, \mathcal{I}_k^\diamond$ and $\mathcal{I}_{k+1}^\diamond$. Moreover, $\mathcal{I}_k^* \cap \mathcal{I}_k^\diamond$ (resp. $\mathcal{I}_k^* \cap \mathcal{I}_{k+1}^\diamond$) is contained in the interior of \mathcal{I}_k^+ (resp. \mathcal{I}_k^-). $\mathcal{I}_k^* \cap \mathcal{I}_{k+1}^+$ is described in (1), and $\mathcal{I}_k^* \cap \mathcal{I}_{k-1}^-$ is described in (2). When $\theta = \frac{\pi}{3}$, \mathcal{I}_k^* will be tangent with \mathcal{I}_{k+1}^+ (resp. \mathcal{I}_{k-1}^-) on $\partial\mathbb{H}_\mathbb{C}^2$ at the parabolic fixed point of $T^k(S^2T^{-1})T^{-k}$ (resp. $T^k(T^{-1}S^2)T^{-k}$).
- (4) \mathcal{I}_k^\diamond is contained in the exterior of all the isometric spheres in \mathcal{S} except $\mathcal{I}_k^\pm, \mathcal{I}_{k-1}^\pm, \mathcal{I}_k^*$ and \mathcal{I}_{k-1}^* . Moreover, $\mathcal{I}_k^\diamond \cap \mathcal{I}_k^*$ and $\mathcal{I}_k^\diamond \cap \mathcal{I}_{k-1}^*$ are described in (3). $\mathcal{I}_k^\diamond \cap \mathcal{I}_k^-$ is described in (2) and $\mathcal{I}_k^\diamond \cap \mathcal{I}_{k-1}^+$ is described in (1). When $\theta = \frac{\pi}{3}$, \mathcal{I}_k^\diamond will be tangent with \mathcal{I}_{k+1}^+ (resp. \mathcal{I}_{k-1}^-) on $\partial\mathbb{H}_\mathbb{C}^2$ at the parabolic fixed point of $T^k(T^{-1}S^2)T^{-k}$ (resp. $T^k(S^2T^{-1})T^{-k}$).

4.3 The Ford domain

Definition 4.12 Let D be the intersection of the closures of the exteriors of the isometric spheres $\mathcal{I}_k^+, \mathcal{I}_k^-, \mathcal{I}_k^*$ and \mathcal{I}_k^\diamond , for $k \in \mathbb{Z}$.

Definition 4.13 For $k \in \mathbb{Z}$, let s_k^+ (resp. s_k^-, s_k^* and s_k^\diamond) be the side of D contained in the isometric sphere \mathcal{I}_k^+ (resp. $\mathcal{I}_k^-, \mathcal{I}_k^*$ and \mathcal{I}_k^\diamond).

Definition 4.14 A ridge is defined to be the 2-dimensional connected intersections of two sides.

By Corollary 4.11, the ridges are $s_k^+ \cap s_k^-$, $s_k^+ \cap s_k^*$, $s_k^+ \cap s_{k-1}^-$, $s_k^+ \cap s_k^\diamond$, $s_k^- \cap s_k^*$ and $s_{k-1}^- \cap s_k^\diamond$ for $k \in \mathbb{Z}$, and the sides and ridges are related as follows:

- The side s_k^+ is bounded by the ridges $s_k^+ \cap s_k^-$, $s_k^+ \cap s_k^*$, $s_k^+ \cap s_{k-1}^-$ and $s_k^+ \cap s_k^\diamond$.
- The side s_k^- is bounded by the ridges $s_k^+ \cap s_k^-$, $s_k^- \cap s_k^*$, $s_k^- \cap s_{k+1}^+$ and $s_0^- \cap s_{k+1}^\diamond$.
- The side s_k^* is bounded by the ridges $s_k^+ \cap s_k^*$ and $s_k^- \cap s_k^*$.
- The side s_k^\diamond is bounded by the ridges $s_k^\diamond \cap s_{k-1}^-$ and $s_k^+ \cap s_k^\diamond$.

Proposition 4.15 *The ridges $s_k^+ \cap s_k^-$, $s_k^+ \cap s_k^*$, $s_k^+ \cap s_{k-1}^-$, $s_k^+ \cap s_k^\diamond$, $s_k^- \cap s_k^*$ and $s_{k-1}^- \cap s_k^\diamond$ for $k \in \mathbb{Z}$ are all topologically the union of two sectors.*

Proof The ridge $s_k^+ \cap s_k^-$ is contained in $\mathcal{I}_k^+ \cap \mathcal{I}_k^-$. According to Proposition 4.10, $\mathcal{I}_k^+ \cap \mathcal{I}_k^-$ is topologically a disc and $\mathcal{I}_k^+ \cap \mathcal{I}_k^- \cap \mathcal{I}_k^*$ is the union of two crossed geodesics. The two crossed geodesics divide the disc into four sectors, one opposite pair of which will lie in the interior of the isometric sphere \mathcal{I}_k^* . Thus $s_k^+ \cap s_k^-$ is the other opposite pair of the four sectors in the disc. More precisely, up to the powers of T , let us consider $s_0^+ \cap s_0^-$. Let Δ be the disc $\mathcal{I}_0^+ \cap \mathcal{I}_0^-$ described in (4-13) and the two crossed geodesics $\mathcal{L}_1 \cup \mathcal{C}_1 \cup \mathcal{C}_2$ be as described in Proposition 4.10. By Proposition 4.2, the complex involution I_2 preserves Δ and $\mathcal{L}_1 \cup \mathcal{C}_1 \cup \mathcal{C}_2$. Recall that I_2 fixes the complex line \mathcal{C}_2 with polar vector n_2 described in Section 3. One can compute that the intersection $\mathcal{C}_2 \cap \Delta$ is the curve

$$(4-16) \quad \mathcal{C}_2 \cap \Delta = \{q(\alpha, \frac{1}{2}\alpha + \theta, \frac{\sqrt{2}}{2}) \in \mathcal{I}_0^+ : \cos(\alpha) \geq \frac{1}{3}\}.$$

Of course $\mathcal{C}_2 \cap \Delta$ intersects with $\mathcal{L}_1 \cup \mathcal{C}_1 \cup \mathcal{C}_2$ at the fixed point of S , and divides Δ into two parts. I_2 fixes $\mathcal{C}_2 \cap \Delta$ and interchanges \mathcal{L}_1 and $\mathcal{C}_1 \cup \mathcal{C}_2$. Thus $\mathcal{C}_2 \cap \Delta$ is contained in the union of two opposite sectors. By Lemma 4.4, $\mathcal{C}_2 \cap \Delta$ lies on the closure of the exterior of \mathcal{I}_0^* , since $f_0^*(\alpha, \frac{1}{2}\alpha + \theta, \frac{\sqrt{2}}{2}) = 1 - \cos(\alpha) \geq 0$. Therefore, the union of two opposite sectors containing $\mathcal{C}_2 \cap \Delta$ is the ridge $s_0^+ \cap s_0^-$. Moreover, this ridge is preserved by I_2 . By using the parametrization of the Giraud disk in [8], we can draw the Giraud disk $\mathcal{I}_0^+ \cap \mathcal{I}_0^-$ and the intersection with the isometric spheres \mathcal{I}_{-1}^- , \mathcal{I}_0^* , \mathcal{I}_{-1}^* , \mathcal{I}_0^\diamond and \mathcal{I}_1^\diamond ; see Figure 4.

The other ridges can be described by a similar argument. □

Proposition 4.16 (1) *The side s_k^+ (resp. s_k^-) is a topological solid cylinder in $\mathbb{H}_{\mathbb{C}}^2 \cup \partial\mathbb{H}_{\mathbb{C}}^2$. The intersection of ∂s_k^+ (resp. ∂s_k^-) with $\mathbb{H}_{\mathbb{C}}^2$ is the disjoint union of two topological discs.*

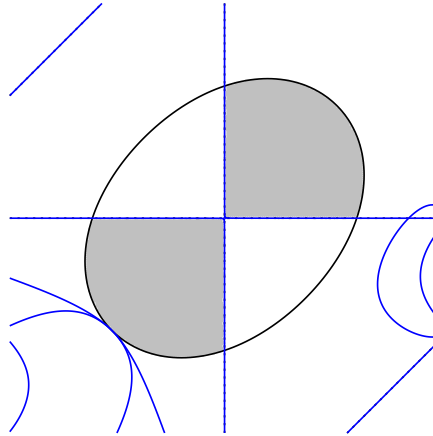


Figure 4: The ridge $s_0^+ \cap s_0^-$ (the shaded region in the intersection of $\mathcal{I}_0^+ \cap \mathcal{I}_0^-$) in the plane with spinal coordinates introduced in [8]. The triple intersection $\mathcal{I}_0^+ \cap \mathcal{I}_0^- \cap \mathcal{I}_0^*$ is the two mutually perpendicular lines. Compare to [8, Figure 16].

- (2) The side s_k^* (resp. s_k^\diamond) is a topological solid light cone in $\mathbb{H}_\mathbb{C}^2 \cup \partial\mathbb{H}_\mathbb{C}^2$. The intersection of ∂s_k^* (resp. ∂s_k^\diamond) with $\mathbb{H}_\mathbb{C}^2$ is the light cone.

Proof (1) The side s_k^+ is contained in the isometric sphere \mathcal{I}_k^+ . By Corollary 4.11, s_k^+ might intersect with the sides contained in the isometric spheres $\mathcal{I}_k^-, \mathcal{I}_{k-1}^-, \mathcal{I}_k^*, \mathcal{I}_{k-1}^*, \mathcal{I}_k^\diamond$ and $\mathcal{I}_{k+1}^\diamond$.

Let Δ_1 be the union of the ridges $s_k^+ \cap s_k^-$ and $s_k^+ \cap s_k^*$, and Δ_2 be the union of the ridges $s_k^+ \cap s_{k-1}^-$ and $s_k^+ \cap s_k^\diamond$. By Proposition 4.10, Δ_1 contains the cross $\mathcal{I}_k^+ \cap \mathcal{I}_k^- \cap \mathcal{I}_k^*$. By Proposition 4.15, Δ_1 is a union of four sectors which are patched together along the cross. Hence, Δ_1 is topologically either a disc or a light cone. By a straightforward computation, the ideal boundary of Δ_1 on $\mathbb{H}_\mathbb{C}^2$ is a simple closed curve on the ideal boundary of \mathcal{I}_k^+ ; see Figure 2. Thus Δ_1 is a topological disc. By a similar argument, Δ_2 is a topological disc.

If $\theta \neq \frac{\pi}{3}$ then $\mathcal{I}_k^+ \cap \mathcal{I}_k^* \cap \mathcal{I}_{k-1}^- = \emptyset$, so Δ_1 and Δ_2 are disjoint, and if $\theta = \frac{\pi}{3}$ they intersect at two points on $\partial\mathbb{H}_\mathbb{C}^2$; see Figures 9 and 10. Note that isometric spheres are topological balls and their pairwise intersections are connected. So, s_k^+ is a topological solid cylinder; see Figure 5. A similar argument describes s_k^- .

- (2) The side s_k^* is contained in the isometric sphere \mathcal{I}_k^* . According to Corollary 4.11, s_k^* only intersects with s_k^+ and s_k^- . Let Δ_3 be the union of $s_k^+ \cap s_k^*$ and $s_k^- \cap s_k^*$. By

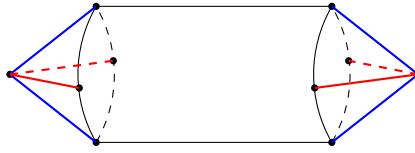


Figure 5: A schematic view of the side s_k^+ (s_k^-).

Propositions 4.10 and 4.15, Δ_3 is a union of four sectors which are patched together along the cross $\mathcal{I}_k^+ \cap \mathcal{I}_k^- \cap \mathcal{I}_k^*$. By a computation for the case $k = 0$, one can see that the ideal boundary of Δ_3 is a union of two disjoint simple closed curves in the ideal boundary of \mathcal{I}_k^* ; see Figure 2. Thus Δ_3 is a light cone. Hence, s_k^* is topologically a solid light cone; see Figure 6. A similar argument describes s_k^\diamond . \square

By applying a Poincaré polyhedron theorem in $\mathbb{H}_{\mathbb{C}}^2$ as stated for example in [22], [8] or [19] (see [3] for a version in the hyperbolic plane), we have our main result:

Theorem 4.17 *Suppose that $\theta \in [0, \frac{\pi}{3}]$. Let D be as in Definition 4.12. Then D is a fundamental domain for the cosets of $\langle T \rangle$ in Γ . Moreover, Γ is discrete and has the presentation*

$$\Gamma = \langle S, T \mid S^4 = (T^{-1}S)^4 = \text{id} \rangle.$$

Proof The sides of D are s_k^+ , s_k^- , s_k^* and s_k^\diamond . The ridges of D are $s_k^+ \cap s_k^-$, $s_k^+ \cap s_k^*$, $s_k^+ \cap s_{k-1}^-$, $s_k^+ \cap s_k^\diamond$, $s_k^- \cap s_k^*$ and $s_{k-1}^- \cap s_k^\diamond$. To obtain the side-pairing maps and ridge cycles, by applying powers of T , it suffices to consider the case where $k = 0$.

The side-pairing maps The side s_0^+ is contained in the isometric sphere $\mathcal{I}(S)$ and s_0^- in the isometric sphere $\mathcal{I}(S^{-1})$. The ridge $s_0^+ \cap s_0^-$ is contained in the disc $\mathcal{I}(S) \cap \mathcal{I}(S^{-1})$, which is defined by the triple equality

$$|\langle z, q_\infty \rangle| = |\langle z, S^{-1}(q_\infty) \rangle| = |\langle z, S(q_\infty) \rangle|$$

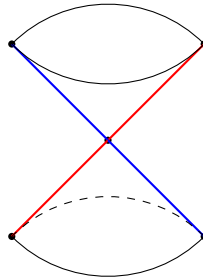


Figure 6: A schematic view of the side s_k^* (s_k^\diamond).

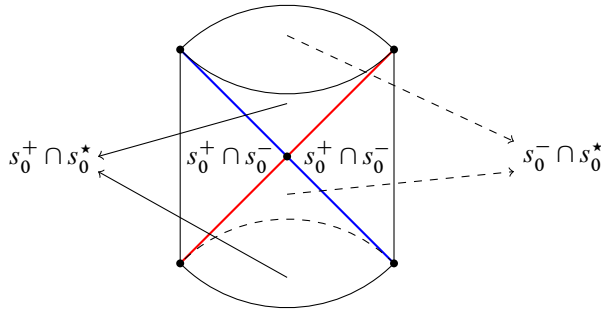


Figure 7: A schematic view of the ridges $s_0^+ \cap s_0^-$, $s_0^+ \cap s_0^*$ and $s_0^- \cap s_0^*$. The thick cross is the triple intersection $\mathcal{I}_0^+ \cap \mathcal{I}_0^- \cap \mathcal{I}_0^*$, that is the union $\mathcal{L}_1 \cup \mathcal{C}_1 \cup \mathcal{C}_2$ described in Proposition 4.10.

and the ridge $s_0^- \cap s_0^*$ is contained in the disc $\mathcal{I}(S^{-1}) \cap \mathcal{I}(S^2)$, which is defined by the triple equality

$$|\langle z, q_\infty \rangle| = |\langle z, S(q_\infty) \rangle| = |\langle z, S^{-2}(q_\infty) \rangle|.$$

Since S maps q_∞ to $S(q_\infty)$, $S^{-1}(q_\infty)$ to q_∞ and $S(q_\infty)$ to $S^2(q_\infty) = S^{-2}(q_\infty)$, S maps the disc $\mathcal{I}(S) \cap \mathcal{I}(S^{-1})$ to the disc $\mathcal{I}(S^{-1}) \cap \mathcal{I}(S^2)$. Note that

$$\mathcal{I}(S) \cap \mathcal{I}(S^{-1}) \cap \mathcal{I}(S^2)$$

is the union of two crossed geodesics (see Proposition 4.10) whose four rays are cyclically permuted by S . Since the ridge $s_0^+ \cap s_0^-$ lies in the closure of the exterior of the isometric sphere $\mathcal{I}(S^2)$, according to (4-16), the point $q(\frac{\pi}{3}, \frac{\pi}{6} + \theta, \frac{\sqrt{2}}{2})$ is contained in $s_0^+ \cap s_0^-$. One can easily verify that $S(q(\frac{\pi}{3}, \frac{\pi}{6} + \theta, \frac{\sqrt{2}}{2}))$ lies in the exterior of $\mathcal{I}(S)$. Thus $S(q(\frac{\pi}{3}, \frac{\pi}{6} + \theta, \frac{\sqrt{2}}{2}))$ is contained in $s_0^- \cap s_0^*$, which lies in the closure of the exterior of the isometric sphere $\mathcal{I}(S)$.

Hence S maps the ridge $s_0^+ \cap s_0^-$ to the ridge $s_0^- \cap s_0^*$. Similarly, S maps $s_0^+ \cap s_0^*$ to $s_0^+ \cap s_0^-$; see Figure 7. Since S maps $\mathcal{I}_0^+ \cap \mathcal{I}_{-1}^- \cap \mathcal{I}_0^\diamond$ to $\mathcal{I}_0^- \cap \mathcal{I}_1^+ \cap \mathcal{I}_1^\diamond$, a similar argument shows that S maps $s_0^+ \cap s_{-1}^-$ to $s_0^- \cap s_1^+$ and $s_0^+ \cap s_0^\diamond$ to $s_0^- \cap s_1^+$.

By a similar argument, s_0^* (resp. s_0^\diamond) is mapped to itself by the elliptic element of order two S^2 (resp. $(T^{-1}S)^2 = (S^{-1}T)^2$), which sends $s_0^+ \cap s_0^*$ to $s_0^- \cap s_0^*$ (resp. $s_0^\diamond \cap s_{-1}^-$ to $s_0^+ \cap s_0^\diamond$) and vice versa.

Hence, the side-pairing maps are

$$T^k S T^{-k} : s_k^+ \rightarrow s_k^-, \quad T^k S^2 T^{-k} : s_k^* \rightarrow s_k^* \quad \text{and} \quad T^k (T^{-1}S)^2 T^{-k} : s_k^\diamond \rightarrow s_k^\diamond.$$

The cycle transformations According to the side-pairing maps, the ridge cycles are

$$(s_k^+ \cap s_k^-, s_k^+, s_k^-) \xrightarrow{T^k S T^{-k}} (s_k^* \cap s_k^-, s_k^*, s_k^-) \xrightarrow{T^k S^2 T^{-k}} (s_k^+ \cap s_k^*, s_k^+, s_k^*) \xrightarrow{T^k S T^{-k}} (s_k^+ \cap s_k^-, s_k^+, s_k^-)$$

and

$$(s_k^+ \cap s_{k-1}^-, s_k^+, s_{k-1}^-) \xrightarrow{T^k (T^{-1} S) T^{-k}} (s_k^\diamond \cap s_{k-1}^-, s_k^\diamond, s_{k-1}^-) \xrightarrow{T^k (T^{-1} S)^2 T^{-k}} (s_k^+ \cap s_k^\diamond, s_k^+, s_k^\diamond) \xrightarrow{T^k (T^{-1} S) T^{-k}} (s_k^+ \cap s_{k-1}^-, s_k^+, s_{k-1}^-).$$

Thus the cycle transformations are

$$T^k S T^{-k} \cdot T^k S^2 T^{-k} \cdot T^k S T^{-k} = T^k S^4 T^{-k}$$

and

$$T^k (T^{-1} S) T^{-k} \cdot T^k (T^{-1} S)^2 T^{-k} \cdot T^k (T^{-1} S) T^{-k} = T^k (T^{-1} S)^4 T^{-k},$$

which are equal to the identity map, since $S^4 = \text{id}$ and $(T^{-1} S)^4 = \text{id}$.

The local tessellation There are exactly two copies of D along each side, since the sides are contained in isometric spheres and the side-pairing maps send the exteriors to the interiors. Thus there is nothing to verify for the points in the interior of every side.

According to the ridge cycles and cycle transformations, there are exactly three copies of D along each ridge.

$s_k^+ \cap s_k^-, s_k^* \cap s_k^-, \text{ and } s_k^+ \cap s_k^*$ These three ridges are in one cycle. Thus, we only need to consider the ridge $s_k^+ \cap s_k^-$. Since the cycle transformation of $s_k^+ \cap s_k^-$ is

$$T^k S T^{-k} \cdot T^k S^2 T^{-k} \cdot T^k S T^{-k} = \text{id},$$

the three copies of D along $s_k^+ \cap s_k^-$ are $D, T^k S^{-1} T^{-k}(D)$ and $T^k S T^{-k}(D)$. We know that $s_k^+ \cap s_k^-$ is contained in $\mathcal{I}(T^k S T^{-k}) \cap \mathcal{I}(T^k S^{-1} T^{-k})$, which is defined by the triple equality

$$|\langle z, \mathbf{q}_\infty \rangle| = |\langle z, T^k S^{-1} T^{-k}(\mathbf{q}_\infty) \rangle| = |\langle z, T^k S T^{-k}(\mathbf{q}_\infty) \rangle|.$$

For z in the neighborhoods of $s_k^+ \cap s_k^-$ in D , $|\langle z, \mathbf{q}_\infty \rangle|$ is the smallest of the three quantities in the above triple equality.

For z in the neighborhoods of $s_k^* \cap s_k^-$ in D , $|\langle z, \mathbf{q}_\infty \rangle|$ is at most $|\langle z, T^k S T^{-k}(\mathbf{q}_\infty) \rangle|$ or $|\langle z, T^k S^{-2} T^{-k}(\mathbf{q}_\infty) \rangle|$. Applying $T^k S^{-1} T^{-k}$ gives a neighborhood of $s_k^+ \cap s_k^-$ in

$T^k S^{-1} T^{-k}(D)$, where $|\langle z, T^k S^{-1} T^{-k}(\mathbf{q}_\infty) \rangle|$ is the smallest of the three quantities in the above triple equality.

For z in the neighborhoods of $s_k^+ \cap s_k^*$ in D , $|\langle z, \mathbf{q}_\infty \rangle|$ is at most $|\langle z, T^k S^{-1} T^{-k}(\mathbf{q}_\infty) \rangle|$ or $|\langle z, T^k S^{-2} T^{-k}(\mathbf{q}_\infty) \rangle|$. Applying $T^k S T^{-k}$ gives a neighborhood of $s_k^+ \cap s_k^-$ in $T^k S T^{-k}(D)$, where $|\langle z, T^k S T^{-k}(\mathbf{q}_\infty) \rangle|$ is the smallest of the three quantities in the above triple equality.

Thus the union of D , $T^k S^{-1} T^{-k}(D)$ and $T^k S T^{-k}(D)$ forms a regular neighborhood of each point in $s_k^+ \cap s_k^-$.

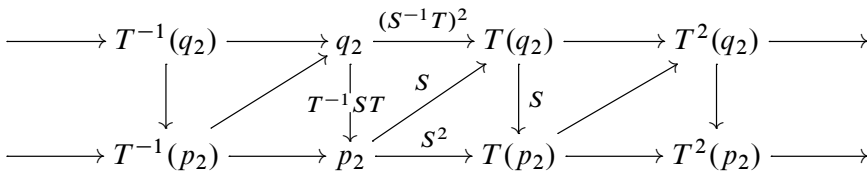
$s_k^+ \cap s_{k-1}^-$, $s_k^\diamond \cap s_{k-1}^-$ and $s_k^+ \cap s_k^\diamond$ We need only consider the ridge $s_k^+ \cap s_{k-1}^-$. Since the cycle transformation of $s_k^+ \cap s_{k-1}^-$ is

$$T^k (T^{-1} S) T^{-k} \cdot T^k (T^{-1} S)^2 T^{-k} \cdot T^k (T^{-1} S) T^{-k} = \text{id},$$

the union of D , $T^k (T^{-1} S)^{-1} T^{-k}(D)$ and $T^k (T^{-1} S) T^{-k}(D)$ forms a regular neighborhood of each point in $s_k^+ \cap s_{k-1}^-$ by a similar argument as in the previous case.

Consistent system of horoballs When $\theta = \frac{\pi}{3}$, there are accidental ideal vertices on D . The sides s_k^* and s_{k+1}^* will be asymptotic on $\partial\mathbb{H}_\mathbb{C}^2$ at the fixed point of the parabolic element $T^k (S^2 T^{-1}) T^{-k}$, and the sides s_k^\diamond and s_{k+1}^\diamond will be asymptotic on $\partial\mathbb{H}_\mathbb{C}^2$ at the fixed point of the parabolic element $T^k (S T^{-1} S) T^{-k}$. To show that there is a consistent system of horoballs it suffices to show that all the cycle transformations fixing a given cusp are nonloxodromic.

Let p_2 be the fixed point of $T^{-1} S^2$ and q_2 be the fixed point of $(T^{-1} S)^2 T$ (the coordinates of p_2 and q_2 are given in Definition 5.1, or see Figure 9). Then all the accidental ideal vertices $\{T^k(p_2)\}$ and $\{T^k(q_2)\}$ are related by the side-pairing maps as follows:



Thus, up to powers of T , all the cycle transformations are $S \cdot S \cdot S^{-2} = \text{id}$ and

$$T^{-1} S T \cdot (S^{-1} T)^{-2} \cdot S = (T^{-1} S^2)^2 = (I_1 I_3 I_2 I_3)^2,$$

which is parabolic. This means that p_2 is fixed by the parabolic element $(T^{-1} S^2)^2$.

Therefore, D is a fundamental domain for the cosets of $\langle T \rangle$ in Γ . The side-pairing maps and T will generate the group Γ . The reflection relations are

$$(T^k S^2 T^{-k})^2 = \text{id} \quad \text{and} \quad (T^k (T^{-1} S)^2 T^{-k})^2 = \text{id}.$$

The cycle relations are

$$T^k S^4 T^{-k} = \text{id} \quad \text{and} \quad T^k (T^{-1} S)^4 T^{-k} = \text{id}.$$

Thus Γ is discrete and has the presentation

$$\Gamma = \langle S, T \mid S^4 = (T^{-1} S)^4 = \text{id} \rangle. \quad \square$$

Since Γ is a subgroup of $\langle I_1, I_2, I_3 \rangle$ of index 2:

Corollary 4.18 *Let $\langle I_1, I_2, I_3 \rangle$ be a complex hyperbolic $(4, 4, \infty)$ triangle group as in Proposition 3.1. Then $\langle I_1, I_2, I_3 \rangle$ is discrete and faithful if and only if $I_1 I_3 I_2 I_3$ is nonelliptic.*

This answers Conjecture 1.1 on the complex hyperbolic $(4, 4, \infty)$ triangle group.

5 The manifold at infinity

In this section, we study the group Γ in the case when $\theta = \frac{\pi}{3}$. That is, the group $\Gamma = \langle S, T \rangle = \langle I_2 I_3, I_2 I_1 \rangle$ with $T^{-1} S^2 = I_1 I_3 I_2 I_3$ being parabolic.

In this case, the Ford domain D has additional ideal vertices on $\partial \mathbb{H}_{\mathbb{C}}^2$, which are parabolic fixed points corresponding to the conjugators of $T^{-1} S^2$. By intersecting a fundamental domain for $\langle T \rangle$ acting on $\partial \mathbb{H}_{\mathbb{C}}^2$ with the ideal boundary of D , we obtain a fundamental domain for Γ acting on its discontinuity region $\Omega(\Gamma)$.

Topologically, this fundamental domain is the product of an unknotted cylinder and a ray; see Proposition 5.13. By cutting and gluing we obtain two polyhedra \mathcal{P}_+ and \mathcal{P}_- ; see Proposition 5.18. Gluing \mathcal{P}_- to \mathcal{P}_+ by S^{-1} , we obtain a polyhedron \mathcal{P} . By studying the combinatorial properties of \mathcal{P} , we show that the quotient $\Omega(\Gamma)/\Gamma$ is homeomorphic to the two-cusped hyperbolic 3-manifold $s782$.

Let U be the ideal boundary of D on $\partial \mathbb{H}_{\mathbb{C}}^2$. Let \tilde{s}_k^+ (resp. \tilde{s}_k^- , \tilde{s}_k^* , and \tilde{s}_k^\diamond) be the ideal boundary of the side of D contained in the ideal boundary of the isometric sphere \mathcal{I}_k^+ (resp. \mathcal{I}_k^- , \mathcal{I}_k^* and \mathcal{I}_k^\diamond). Then the union of all the sides $\{\tilde{s}_k^+\}$, $\{\tilde{s}_k^-\}$, $\{\tilde{s}_k^*\}$ and $\{\tilde{s}_k^\diamond\}$ for $k \in \mathbb{Z}$ form the boundary of U .

5.1 The vertices of U

Definition 5.1 In the Heisenberg coordinates we define the points

$$\begin{aligned}
 q_2 &= \left[\frac{1}{2}(-3+i\sqrt{3}), -\sqrt{3} \right], & p_6 &= \left[\frac{1}{6}(2-\sqrt{6}+i(2\sqrt{3}+\sqrt{2})), -\frac{4}{3}\sqrt{2} \right], \\
 q_3 &= \left[\frac{1}{2}(1+i\sqrt{3}), \sqrt{3} \right], & p_7 &= \left[\frac{1}{6}(2+\sqrt{6}+i(2\sqrt{3}-\sqrt{2})), \frac{4}{3}\sqrt{2} \right], \\
 p_2 &= \left[\frac{1}{2}(-1+i\sqrt{3}), -\sqrt{3} \right], & p_8 &= \left[\frac{1}{6}(-2+\sqrt{6}+i(2\sqrt{3}+\sqrt{2})), \frac{4}{3}\sqrt{2} \right], \\
 p_3 &= \left[\frac{1}{2}(3+i\sqrt{3}), \sqrt{3} \right], & p_9 &= \left[\frac{1}{6}(-2-\sqrt{6}+i(2\sqrt{3}-\sqrt{2})), -\frac{4}{3}\sqrt{2} \right], \\
 p_4 &= \left[\frac{1}{6}(4+\sqrt{6}+i(4\sqrt{3}-\sqrt{2})), 0 \right], & p_{10} &= \left[\frac{1}{6}(-4+\sqrt{6}+i(4\sqrt{3}+\sqrt{2})), 0 \right], \\
 p_5 &= \left[\frac{1}{6}(4-\sqrt{6}+i(4\sqrt{3}+\sqrt{2})), 0 \right], & p_{11} &= \left[\frac{1}{6}(-4-\sqrt{6}+i(4\sqrt{3}-\sqrt{2})), 0 \right],
 \end{aligned}$$

and

$$p_{12} = T(p_9), \quad p_{13} = T(p_8), \quad p_{14} = T(p_{11}), \quad p_{15} = T(p_{10}).$$

By Proposition 4.10 and Corollary 4.11, we have the following:

Proposition 5.2 *The points in Definition 5.1 satisfy:*

- p_4, p_5, p_6 and p_7 are the four points on the ideal boundary of $\mathcal{I}_0^+ \cap \mathcal{I}_0^- \cap \mathcal{I}_0^*$, which is described in Proposition 4.10.
- p_8, p_9, p_{10} and p_{11} are the four points on the ideal boundary of $\mathcal{I}_0^+ \cap \mathcal{I}_{-1}^- \cap \mathcal{I}_0^\diamond$.
- p_{12}, p_{13}, p_{14} and p_{15} are the four points on the ideal boundary of $\mathcal{I}_1^+ \cap \mathcal{I}_0^- \cap \mathcal{I}_1^\diamond$.
- p_2 (resp. p_3) is the parabolic fixed point of $T^{-1}S^2$ (resp. S^2T^{-1}), which is the intersection $\mathcal{I}_0^+ \cap \mathcal{I}_{-1}^- \cap \mathcal{I}_0^* \cap \mathcal{I}_{-1}^*$ (resp. $\mathcal{I}_1^+ \cap \mathcal{I}_0^- \cap \mathcal{I}_0^* \cap \mathcal{I}_1^*$).
- q_3 (resp. q_2) is the parabolic fixed point of $ST^{-1}S$ (resp. $T^{-1}ST^{-1}ST$), which is the intersection of the four isometric spheres $\mathcal{I}_0^+ \cap \mathcal{I}_0^- \cap \mathcal{I}_0^\diamond \cap \mathcal{I}_1^\diamond$ (resp. $\mathcal{I}_{-1}^+ \cap \mathcal{I}_{-1}^- \cap \mathcal{I}_0^\diamond \cap \mathcal{I}_{-1}^\diamond$).

Proof As described in Proposition 4.10, all of the triple intersections $\mathcal{I}_0^+ \cap \mathcal{I}_0^- \cap \mathcal{I}_0^*$, $\mathcal{I}_0^+ \cap \mathcal{I}_{-1}^- \cap \mathcal{I}_0^\diamond$ and $\mathcal{I}_1^+ \cap \mathcal{I}_0^- \cap \mathcal{I}_1^\diamond$ have exactly four points lying on $\partial\mathbb{H}_\mathbb{C}^2$. When writing the standard lifts of p_4, p_5, p_6 and p_7 , one can see that they are the four points in the proof of Proposition 4.10. Thus the first item is proved.

By Proposition 4.2, the four points of $\mathcal{I}_0^+ \cap \mathcal{I}_{-1}^- \cap \mathcal{I}_0^\diamond$ are the images of p_4, p_5, p_6 and p_7 under the antiholomorphic involution τ , which are p_{11}, p_{10}, p_8 and p_9 .

The second item and the fact that $\mathcal{I}_1^+ \cap \mathcal{I}_0^- \cap \mathcal{I}_1^\diamond = T(\mathcal{I}_0^+ \cap \mathcal{I}_{-1}^- \cap \mathcal{I}_0^\diamond)$ imply the third item.

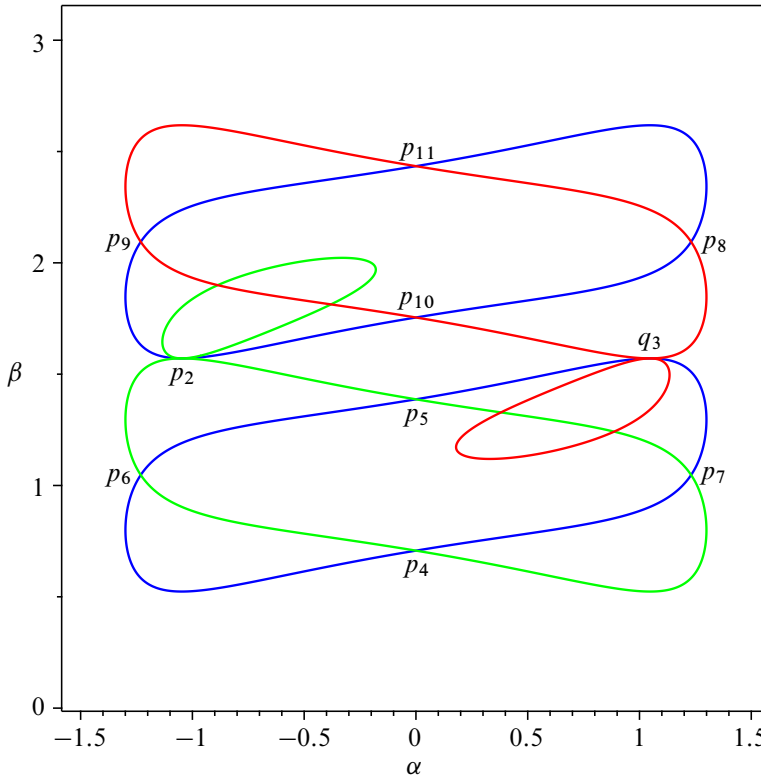


Figure 8: Intersections of the isometric spheres $\mathcal{I}_0^-, \mathcal{I}_{-1}^-, \mathcal{I}_0^*, \mathcal{I}_{-1}^*, \mathcal{I}_0^\diamond$ and \mathcal{I}_1^\diamond with \mathcal{I}_0^+ in $\partial\mathbb{H}_\mathbb{C}^2$, viewed in geographical coordinates. Here $\alpha \in [-\frac{\pi}{2}, \frac{\pi}{2}]$ in the vertical coordinate and $\beta \in [0, \pi]$ in the horizontal one. The region exterior to the six Jordan closed curves has two connect components. One of them is the topological octagon with vertices $p_2, p_6, p_4, p_7, q_3, p_8, p_{11}$ and p_9 . The other one is a topological quadrilateral with vertices p_2, p_5, q_3 and p_{10} .

We will only prove the statement for p_2 in the last two items; the others follow by similar arguments. By Lemma 4.8, p_2 is the parabolic fixed point of $T^{-1}S^2$ and is the triple intersection $\mathcal{I}_0^+ \cap \mathcal{I}_{-1}^- \cap \mathcal{I}_0^*$. By Corollary 4.11(3), \mathcal{I}_0^* is tangent with \mathcal{I}_{-1}^* at p_2 . \square

5.2 The sides of U

Now we study the combinatorial properties of the sides; see Figures 8 and 9.

Proposition 5.3 *The interior of the side \tilde{s}_0^+ has connected components*

- an octagon, denoted by \mathcal{O}_0^+ , with vertices $p_2, p_6, p_4, p_7, q_3, p_8, p_{11}$ and p_9 ,
- a quadrilateral, denoted by \mathcal{Q}_0^+ , with vertices p_2, p_5, q_3 and p_{10} .

Proof By Proposition 4.16, when $\theta < \frac{\pi}{3}$, the side \tilde{s}_0^+ is topologically an annulus bounded by two disjoint simple closed curves which are the union of the ideal boundaries of the ridges $s_0^+ \cap s_{-1}^-$ and $s_0^+ \cap s_0^\diamond$, respectively $s_0^+ \cap s_0^-$ and $s_0^+ \cap s_0^*$. When $\theta = \frac{\pi}{3}$, these two curves intersect at two points, which divide \tilde{s}_0^+ into two parts. That is to say the interior of the side \tilde{s}_0^+ has two connected components.

By Proposition 5.2, the ideal boundary of the ridge $s_0^+ \cap s_{-1}^-$ (resp. $s_0^+ \cap s_0^\diamond$) is a union of two disjoint Jordan arcs $[p_9, p_{10}]$ and $[p_8, p_{11}]$ (resp. $[p_{10}, p_8]$ and $[p_{11}, p_9]$), and the ideal boundary of the ridge $s_0^+ \cap s_0^-$ (resp. $s_0^+ \cap s_0^*$) is a union of two disjoint Jordan arcs $[p_5, p_7]$ and $[p_4, p_6]$ (resp. $[p_7, p_4]$ and $[p_6, p_5]$). Since p_2 is the intersection of four isometric spheres $\mathcal{I}_0^+ \cap \mathcal{I}_{-1}^- \cap \mathcal{I}_0^* \cap \mathcal{I}_{-1}^*$, it lies on $[p_9, p_{10}]$ and $[p_6, p_5]$. Similarly, q_3 lies on $[p_5, p_7]$ and $[p_{10}, p_8]$.

By Proposition 4.2, the antiholomorphic involution τ preserves \tilde{s}_0^+ and interchanges its boundaries. It is easy to check that τ interchanges p_2 and q_3 , p_5 and p_{10} , p_4 and p_{11} , p_6 and p_8 , and p_7 and p_9 . Thus one part of \tilde{s}_0^+ is a quadrilateral with vertices p_2, p_5, q_3 and p_{10} , denoted by \mathcal{O}_0^+ . The other is an octagon with vertices $p_2, p_6, p_4, p_7, q_3, p_8, p_{11}$ and p_9 , denoted by \mathcal{Q}_0^+ . Both of them are preserved by τ . □

According to the symmetry I_2 in Proposition 4.2, which interchanges \mathcal{I}_0^+ and \mathcal{I}_0^- :

Proposition 5.4 *The interior of the side \tilde{s}_0^- has connected components*

- an octagon, denoted by \mathcal{O}_0^- , with vertices $p_5, p_6, p_4, p_3, p_{15}, p_{13}, p_{14}$ and q_3 ,
- a quadrilateral, denoted by \mathcal{Q}_0^- , with vertices p_3, p_7, q_3 and p_{12} .

Proof Note that side s_0^- is bounded by the ridges $s_0^- \cap s_1^+, s_0^- \cap s_1^\diamond, s_0^- \cap s_0^+$ and $s_0^- \cap s_0^*$. By Proposition 4.2, the side s_0^- is isometric to s_0^+ under the complex involution I_2 . Thus its ideal boundary \tilde{s}_0^- will be also isometric to \tilde{s}_0^+ . This implies that \tilde{s}_0^- has the same combinatorial properties as \tilde{s}_0^+ . One can check that

$$I_2: (q_3, p_5, p_2, p_{10}, p_8, p_{11}, p_9, p_6) \leftrightarrow (q_3, p_7, p_3, p_{12}, p_{14}, p_{13}, p_{15}, p_4).$$

Thus one part of \tilde{s}_0^- is an octagon, denoted by \mathcal{O}_0^- , whose vertices are $p_5, p_6, p_4, p_3, p_{15}, p_{13}, p_{14}$ and q_3 . The other is a quadrilateral, denoted by \mathcal{Q}_0^- , whose vertices are p_3, p_7, q_3 and p_{12} ; see Figure 9. □

Remark 5.5 The vertex q_3 lies on the \mathbb{C} -circle associated to I_2 , that is, the ideal boundary of the complex line fixed by I_2 . One can also observe that p_2 is fixed by I_1 .

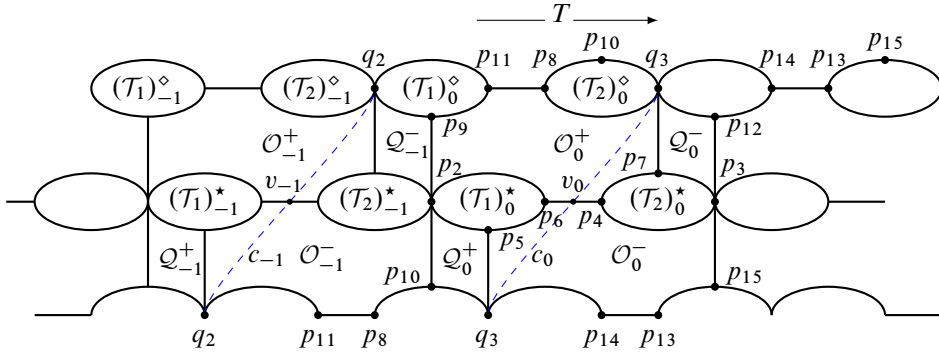


Figure 9: A combinatorial picture of ∂U . The top and bottom curves are identified. \mathcal{O}_0^{\pm} (resp. \mathcal{O}_{-1}^{\pm}) is divided by c_0 (resp. c_{-1}) into a quadrilateral \mathcal{Q}_0^{\pm} (resp. \mathcal{Q}_{-1}^{\pm}) and a heptagon \mathcal{H}_0^{\pm} (resp. \mathcal{H}_{-1}^{\pm}), v_0 is the intersection of c_0 with the arc $[p_4, p_6]$ and v_{-1} is the intersection of c_{-1} with the arc $[T^{-1}(p_4), T^{-1}(p_6)]$.

Proposition 5.6 *The interior of side \tilde{s}_0^{\star} is a union of two disjoint triangles, denoted by $(\mathcal{T}_1)_0^{\star}$ and $(\mathcal{T}_2)_0^{\star}$, whose vertices are p_2, p_5 and p_6 and p_3, p_4 and p_7 , respectively.*

Proof By Proposition 4.16, the side \tilde{s}_0^{\star} is the union of two disjoint discs, which are bounded by the ideal boundary of the ridges $s_0^+ \cap s_0^{\star}$ and $s_0^- \cap s_0^{\star}$.

As stated in Proposition 5.2, the ideal boundary of $\mathcal{I}_0^+ \cap \mathcal{I}_0^- \cap \mathcal{I}_0^{\star}$ contains the four points p_4, p_5, p_6 and p_7 . Thus \tilde{s}_0^{\star} is the union of two disjoint bigons, one with vertices p_5 and p_6 , and the other with p_4 and p_7 . Proposition 5.2 also tells us that p_2 and p_3 lie on different components of the boundaries of the two bigons.

Therefore, both of the components are triangles, denoted by $(\mathcal{T}_1)_0^{\star}$ and $(\mathcal{T}_2)_0^{\star}$, whose vertices are p_2, p_5 and p_6 and p_3, p_4 and p_7 , respectively. □

According to the symmetry τ in Proposition 4.2, the side \tilde{s}_0^{\diamond} has the same topological properties as the side \tilde{s}_0^{\star} . Thus by a similar argument:

Proposition 5.7 *The interior of side \tilde{s}_0^{\diamond} is a union of two disjoint triangles, denoted by $(\mathcal{T}_1)_0^{\diamond}$ and $(\mathcal{T}_2)_0^{\diamond}$, whose vertices are q_2, p_9 and p_{11} , and q_3, p_8 and p_{10} , respectively.*

5.3 A fundamental domain for the subgroup $\langle T \rangle$

Proposition 5.8 *Let $L = \{[x + i\frac{\sqrt{3}}{2}, \sqrt{3}x] \in \mathcal{N} : x \in \mathbb{R}\}$. Then L is a T -invariant \mathbb{R} -circle. Furthermore, L is contained in the complement of D .*

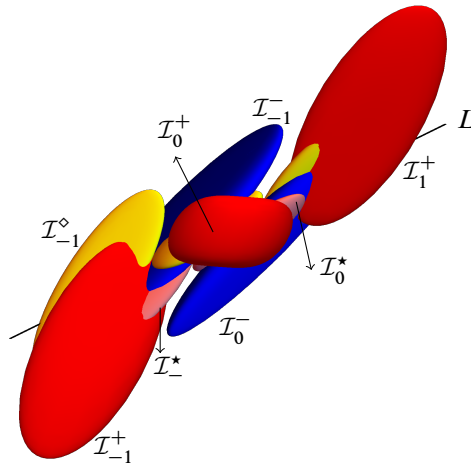


Figure 10: A realistic picture of the ideal boundaries of the isometric spheres. \mathcal{I}_0^+ , \mathcal{I}_1^+ and \mathcal{I}_{-1}^+ (red), \mathcal{I}_0^- and \mathcal{I}_{-1}^- (blue), \mathcal{I}_0^* and \mathcal{I}_{-1}^* (pink), \mathcal{I}_0^\diamond , $\mathcal{I}_{-1}^\diamond$ and $\mathcal{I}_{-1}^\diamond$ (yellow). The line L is the T -invariant \mathbb{R} -circle.

Proof It is obvious that L is an \mathbb{R} -circle, since it is the image of the x -axis of \mathcal{N} by a Heisenberg translation along the y -axis. For any point $[x + i\frac{\sqrt{3}}{2}, \sqrt{3}x] \in L$, we have $T([x + i\frac{\sqrt{3}}{2}, \sqrt{3}x]) = [(x + 2) + i\frac{\sqrt{3}}{2}, \sqrt{3}(x + 2)]$, which lies in L . Thus L is a T -invariant \mathbb{R} -circle; see Figure 10.

Note that T acts on L as a translation through 2. To show L is contained in the complement of D , it suffices to show that a segment with length 2 is contained in the interior of some isometric spheres. By considering the Cygan distance between a point in L and the center of an isometric sphere, one can compute that the segments $\{[x + i\frac{\sqrt{3}}{2}, \sqrt{3}x] : -\frac{1}{2} \leq x \leq \frac{1}{2}\}$ and $\{[x + i\frac{\sqrt{3}}{2}, \sqrt{3}x] : \frac{1}{2} \leq x \leq \frac{3}{2}\}$ lie in the interiors of \mathcal{I}_0^+ and \mathcal{I}_0^- , respectively. □

Definition 5.9 Let

$$\Sigma_{-1} = \{[-\frac{3}{2} + iy, t] \in \mathcal{N} : y, t \in \mathbb{R}\} \quad \text{and} \quad \Sigma_0 = \{[\frac{1}{2} + iy, t] \in \mathcal{N} : y, t \in \mathbb{R}\}$$

be two planes in the Heisenberg group.

In fact, the vertical planes Σ_{-1} and Σ_0 are boundaries of *fans* in the sense of [14]. Let D_T be the region between Σ_{-1} and Σ_0 , that is

$$D_T = \{[x + iy, t] \in \mathcal{N} : -\frac{3}{2} \leq x \leq \frac{1}{2}\}.$$

It is clear that $\Sigma_0 = T(\Sigma_{-1})$. Thus D_T is a fundamental domain for $\langle T \rangle$ acting on $\partial\mathbb{H}_{\mathbb{C}}^2$.

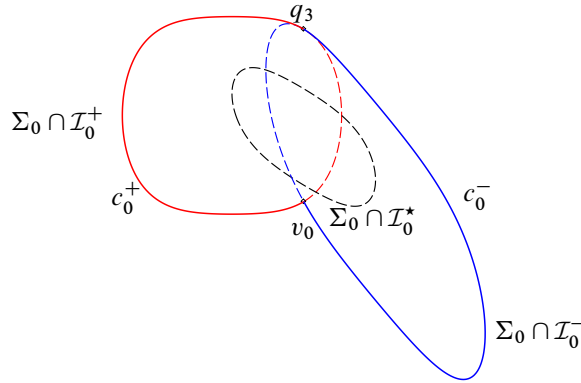


Figure 11: The intersection of Σ_0 with \mathcal{I}_0^+ , \mathcal{I}_0^- and \mathcal{I}_0^* viewed in Σ_0 . Here $c_0 = c_0^+ \cup c_0^-$ is a simple closed curve, where c_0^+ and c_0^- are the solid line parts of $\Sigma_0 \cap \mathcal{I}_0^+$ and $\Sigma_0 \cap \mathcal{I}_0^-$, respectively.

Proposition 5.10 *The intersections of Σ_0 and Σ_{-1} with the isometric spheres \mathcal{I}_k^\pm , \mathcal{I}_k^* and \mathcal{I}_k^\diamond are empty, except:*

- $\Sigma_0 \cap \mathcal{I}_0^\pm$ and $\Sigma_0 \cap \mathcal{I}_0^*$ are circles, and $\Sigma_0 \cap \mathcal{I}_0^\diamond = \Sigma_0 \cap \mathcal{I}_1^\diamond = \{q_3\}$.
- $\Sigma_{-1} \cap \mathcal{I}_{-1}^\pm$ and $\Sigma_{-1} \cap \mathcal{I}_{-1}^*$ are circles, and $\Sigma_{-1} \cap \mathcal{I}_{-1}^\diamond = \Sigma_{-1} \cap \mathcal{I}_0^\diamond = \{q_2\}$.

Proof Since the isometric spheres are strictly convex, their intersections with a plane are either a topological circle, a point or empty. Note that $\Sigma_0 = T(\Sigma_{-1})$. Thus it suffices to consider the intersections of Σ_0 with the isometric spheres. By a strait computation, each one of $\Sigma_0 \cap \mathcal{I}_0^\pm$ and $\Sigma_0 \cap \mathcal{I}_0^*$ is a circle; see Figure 11. □

Lemma 5.11 *The plane Σ_0 (resp. Σ_{-1}) is preserved by I_2 (resp. $T^{-1}I_2T$). The intersection $\Sigma_0 \cap \partial U$ (resp. $\Sigma_{-1} \cap \partial U$) is a simple closed curve c_0 (resp. c_{-1}) in the union $\tilde{s}_0^+ \cup \tilde{s}_0^-$ (resp. $\tilde{s}_{-1}^+ \cup \tilde{s}_{-1}^-$), which contains the points q_3 and $v_0 = [\frac{1}{2} + i\frac{\sqrt{3}}{2}, -\sqrt{3}]$ (resp. q_2 and $v_{-1} = T^{-1}(v_0)$).*

Proof It suffices to consider Σ_0 . The \mathbb{C} -circle associated to I_2 , that is, the ideal boundary of the complex line fixed by I_2 , is $\{[\frac{1}{2} + i\frac{\sqrt{3}}{2}, t] \in \mathcal{N} : t \in \mathbb{R}\}$, which is contained in Σ_0 . Thus Σ_0 is preserved by I_2 .

It is obvious that Σ_0 contains q_3 , which is the tangent point of \mathcal{I}_0^\diamond and \mathcal{I}_1^\diamond . The intersections $\Sigma_0 \cap \mathcal{I}_0^+$, $\Sigma_0 \cap \mathcal{I}_0^-$ and $\Sigma_0 \cap \mathcal{I}_0^*$ are circles by Proposition 5.10. One can compute that the intersection $\Sigma_0 \cap \mathcal{I}_0^+ \cap \mathcal{I}_0^-$ contains q_3 , and $v_0 = [\frac{1}{2} + i\frac{\sqrt{3}}{2}, -\sqrt{3}]$; see Figure 11. These two points divide the circles on \mathcal{I}_0^+ and \mathcal{I}_0^- into two arcs. Let c_0^+

be the arc with endpoints q_3 and v_0 on \mathcal{I}_0^+ lying in the exterior of \mathcal{I}_0^- and c_0^- be the one on \mathcal{I}_0^- lying in the exterior of \mathcal{I}_0^+ . Then $c_0 = c_0^+ \cup c_0^-$ is a simple closed curve. Observe that $\Sigma_0 \cap \mathcal{I}_0^*$ lies in the union of the interiors of \mathcal{I}_0^+ and \mathcal{I}_0^- . Thus Σ_0 does not intersect \tilde{s}_0^* . By Proposition 5.10, c_0^+ lies on \tilde{s}_0^+ and c_0^- lies on \tilde{s}_0^- . Therefore, the intersection $\Sigma_0 \cap \partial U$ is c_0 , which is a simple closed curve containing q_3 and v_0 . \square

5.4 The topology of U

Proposition 5.12 *Let U^c be the closure of the complement of U in \mathcal{N} . Then the closure of the intersection $U^c \cap D_T$ is a solid tube homeomorphic to a 3–ball.*

Proof It suffices to show that the boundary of $U^c \cap D_T$ is a 2–sphere. Now let us consider the cell structure of $U^c \cap D_T$; see Figure 9. According to Lemma 5.11, the intersection of U^c with Σ_0 (resp. Σ_{-1}) is a topological disc with two vertices, q_3 and v_0 (resp. q_2 and v_{-1}), and two edges, c_0^\pm (resp. c_{-1}^\pm). Also, c_0 (resp. c_{-1}) divides \mathcal{O}_0^\pm (resp. \mathcal{O}_{-1}^\pm) into a quadrilateral \mathcal{Q}'_0^\pm (resp. \mathcal{Q}'_{-1}^\pm) and a heptagon \mathcal{H}_0^\pm (resp. \mathcal{H}_{-1}^\pm).

Since p_2, p_5 and $T^{-1}(p_4)$ are contained in D_T , one can see that D_T contains $\mathcal{Q}'_0^-, \mathcal{Q}'_{-1}^+, \mathcal{H}_0^+$ and \mathcal{H}_{-1}^- . Besides, D_T contains $\mathcal{Q}_0^+, \mathcal{Q}_{-1}^-, (\mathcal{T}_1)_0^\diamond, (\mathcal{T}_2)_0^\diamond, (\mathcal{T}_1)_0^*$ and $(\mathcal{T}_2)_{-1}^*$. Thus the boundary of $U^c \cap D_T$ consists of 12 faces, 23 edges and 13 vertices; see the region between c_0 and c_{-1} in Figure 9. Therefore the Euler characteristic of the boundary of $U^c \cap D_T$ is 2. So the boundary of $U^c \cap D_T$ is a 2–sphere. \square

Propositions 5.8 and 5.12 imply the following result:

Proposition 5.13 *$U \cap D_T$ is the product of an unknotted cylinder with a ray, which is homeomorphic to $S^1 \times [0, 1] \times \mathbb{R}_{\geq 0}$.*

Proof As stated in Proposition 5.8, U^c contains the line L . Thus $U^c \cap D_T$ is a tubular neighborhood of $L \cap D_T$. It cannot be knotted. Therefore $\partial U \cap D_T$ is an unknotted cylinder homeomorphic to $S^1 \times [0, 1]$. One can see that $U \cap \Sigma_0$ is the product of c_0 with a ray, and $U \cap \Sigma_{-1}$ is the product of c_{-1} with a ray. Both of them are homeomorphic to $S^1 \times \mathbb{R}_{\geq 0}$. Hence $U \cap D_T$ is the product of an unknotted cylinder with a ray, and is homeomorphic to $S^1 \times [0, 1] \times \mathbb{R}_{\geq 0}$. \square

Applying powers of T , Proposition 5.13 immediately implies the following corollary:

Corollary 5.14 *U is the product of an unknotted cylinder with a ray homeomorphic to $S^1 \times \mathbb{R} \times \mathbb{R}_{\geq 0}$.*

Remark 5.15 U is the complement of a tubular neighborhood of the T -invariant \mathbb{R} -circle L , that is, a horotube for T . (See [28] for the definition of a horotube.)

5.5 The manifold

Definition 5.16 Suppose that the cylinder $S^1 \times [0, 1]$ has a combinatorial cell structure with finite faces $\{F_i\}$. A *canonical subdivision* on $S^1 \times [0, 1] \times \mathbb{R}_{\geq 0}$ is a finite union of 3-dimensional pieces $\{\hat{F}_i\}$ where $\hat{F}_i = F_i \times \mathbb{R}_{\geq 0}$.

Proposition 5.17 *There is a canonical subdivision on $U \cap D_T$.*

Proof As described in the proof of Proposition 5.12, the combinatorial cell structure of $\partial U \cap D_T$ has 10 faces, $\mathcal{Q}'_0, \mathcal{Q}'_{-1}, \mathcal{H}_0, \mathcal{H}_{-1}, \mathcal{Q}_0, \mathcal{Q}_{-1}, (\mathcal{T}_1)_0^\diamond, (\mathcal{T}_2)_0^\diamond, (\mathcal{T}_1)_0^\star$ and $(\mathcal{T}_2)_0^\star$. By Proposition 5.13, $U \cap D_T$ is the union of 3-dimensional pieces $\hat{\mathcal{Q}}'^-, \hat{\mathcal{Q}}'^+, \hat{\mathcal{H}}_0, \hat{\mathcal{H}}_{-1}, \hat{\mathcal{Q}}_0, \hat{\mathcal{Q}}_{-1}, (\hat{\mathcal{T}}_1)_0^\diamond, (\hat{\mathcal{T}}_2)_0^\diamond, (\hat{\mathcal{T}}_1)_0^\star$ and $(\hat{\mathcal{T}}_2)_0^\star$. Combinatorially, these 3-dimensional pieces are the cone from q_∞ to the faces of $\partial U \cap D_T$. \square

Let $\Omega(\Gamma)$ be the discontinuity region of Γ acting on $\partial\mathbb{H}^2_{\mathbb{C}}$. Then $U \cap D_T$ is obviously a fundamental domain for Γ . By cutting and gluing, we can obtain the following fundamental domain for Γ acting on $\Omega(\Gamma)$:

Proposition 5.18 *Let \mathcal{P}_+ be the union of $\hat{\mathcal{H}}_0^+, (\hat{\mathcal{T}}_1)_0^\diamond, (\hat{\mathcal{T}}_2)_0^\diamond, T(\hat{\mathcal{Q}}'^+)$, $T(\hat{\mathcal{Q}}'^-)$ and $T((\hat{\mathcal{T}}_2)_0^\star)$. Let \mathcal{P}_- be the union of $\hat{\mathcal{Q}}_0^+, (\hat{\mathcal{T}}_1)_0^\star, \hat{\mathcal{Q}}_0^-$ and $T(\hat{\mathcal{H}}_{-1})$. Then $\mathcal{P}_+ \cup \mathcal{P}_-$ is a fundamental domain for Γ acting on $\Omega(\Gamma)$. Moreover, \mathcal{P}_+ (resp. \mathcal{P}_-) is combinatorially an eleven-pyramid (resp. nine-pyramid) with cone vertex q_∞ and base*

$$\mathcal{O}_0^+ \cup \mathcal{Q}_0^- \cup (\mathcal{T}_1)_0^\diamond \cup (\mathcal{T}_2)_0^\diamond \cup (\mathcal{T}_2)_0^\star \quad (\text{resp. } \mathcal{O}_0^- \cup \mathcal{Q}_0^+ \cup (\mathcal{T}_1)_0^\star).$$

Proof Since $\Sigma_0 = T(\Sigma_{-1})$ and $c_0 = T(c_{-1})$, $U \cap D_T$ and $T(U \cap D_T)$ can be glued together along $c_0 \times \mathbb{R}_{\geq 0}$. Note that $U \cap D_T$ is a fundamental domain for Γ acting on $\Omega(\Gamma)$ and has a subdivision as described in Proposition 5.17. Therefore $\mathcal{P}_+ \cup \mathcal{P}_-$ is also a fundamental domain.

As described in Proposition 5.12, c_0 (resp. c_{-1}) divides \mathcal{O}_0^\pm (resp. \mathcal{O}_{-1}^\pm) into a quadrilateral \mathcal{Q}'_0^\pm (resp. \mathcal{Q}'_{-1}^\pm) and a heptagon \mathcal{H}_0^\pm (resp. \mathcal{H}_{-1}^\pm). Note that $\mathcal{O}_0^\pm = T(\mathcal{O}_{-1}^\pm)$ and $(\mathcal{T}_2)_0^\star = T((\mathcal{T}_2)_{-1}^\star)$. Thus the base of \mathcal{P}_+ (resp. \mathcal{P}_-) is $\mathcal{O}_0^+ \cup \mathcal{Q}_0^- \cup (\mathcal{T}_1)_0^\diamond \cup (\mathcal{T}_2)_0^\diamond \cup (\mathcal{T}_2)_0^\star$ (resp. $\mathcal{O}_0^- \cup \mathcal{Q}_0^+ \cup (\mathcal{T}_1)_0^\star$), which is combinatorially a hendecagon (resp. an enneagon); see Figures 9 and 12. \square

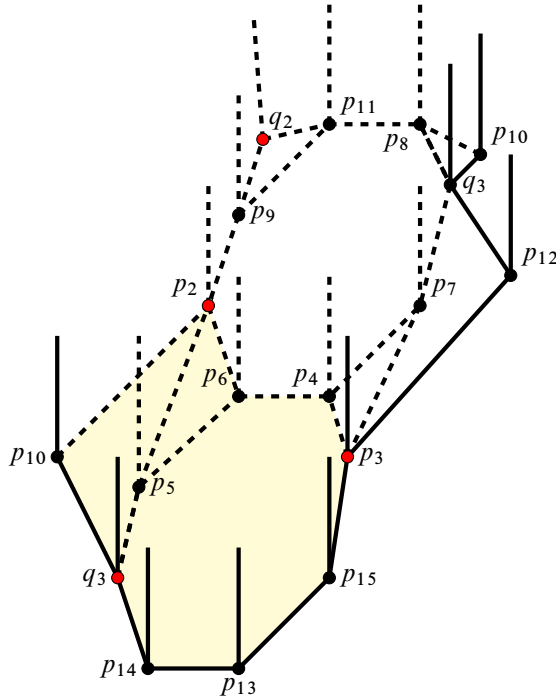


Figure 12: A schematic view of the fundamental domain of Γ on $\Omega(\Gamma)$. The red vertices are the parabolic fixed points. The yellow polygon is $\mathcal{O}_0^- \cup \mathcal{Q}_0^+ \cup (\mathcal{T}_1)_0^*$.

Definition 5.19 Let $p'_2 = S^{-1}(p_2)$, $p_1 = S^{-1}(q_\infty) = [0, 0]$ and $p'_{10} = S^{-1}(p_{10})$.

Lemma 5.20 Let \mathcal{P} be the union $\mathcal{P}_+ \cup S^{-1}(\mathcal{P}_{-1})$. Then \mathcal{P} is combinatorially a polyhedron with 8 triangular faces, 4 square faces, 2 pentagonal faces and 2 hexagonal faces. The faces of \mathcal{P} are paired as

$$\begin{aligned}
 T &: (q_\infty, p_2, p_9, q_2) \mapsto (q_\infty, p_3, p_{12}, q_3), \\
 S^{-1}T &: (q_\infty, q_2, p_{11}, p_8, p_{10}) \mapsto (p_1, p_2, p_9, p_{11}, p_8), \\
 (S^{-1}T)^2 &: (q_2, p_9, p_{11}) \mapsto (q_3, p_8, p_{10}), \\
 S^{-1} &: (q_\infty, p_{10}, q_3) \mapsto (p_1, p'_{10}, p_2), \\
 S^{-1}T^{-1}S &: (p_1, p_8, q_3) \mapsto (p_1, p'_{10}, p'_2), \\
 S^{-2} &: (q_3, p_{12}, p_3, p_7) \mapsto (p'_2, p'_{10}, p_2, p_6), \\
 S^{-1} &: (q_\infty, p_2, p_6, p'_2, p_4, p_3) \mapsto (p_1, p'_2, p_4, p_3, p_7, q_3), \\
 S^{-1} &: (p_6, p'_2, p_4) \mapsto (p_4, p_3, p_7).
 \end{aligned}$$

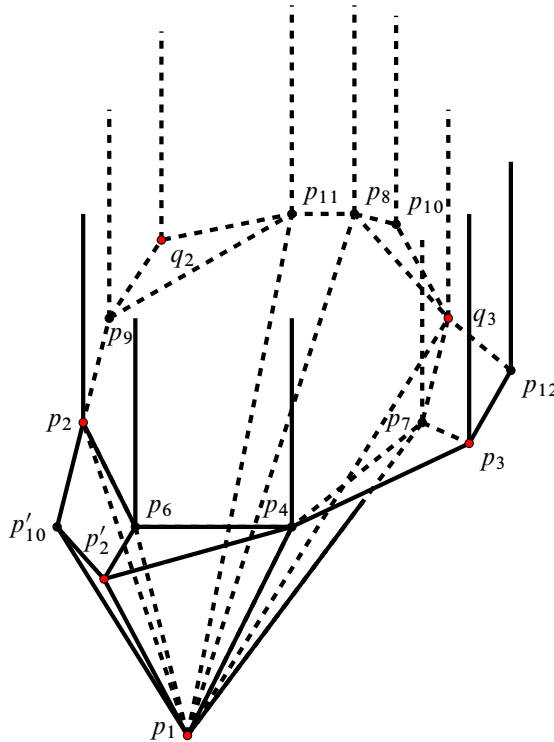


Figure 13: The combinatorial picture of \mathcal{P} . The red vertices of \mathcal{P} are the parabolic fixed points.

Proof The bases of \mathcal{P}_+ and \mathcal{P}_{-1} are paired as

$$\begin{aligned} S: \mathcal{Q}_0^+ &\rightarrow \mathcal{Q}_0^-, & (p_2, p_5, q_3, p_{10}) &\mapsto (q_3, p_7, p_3, p_{12}), \\ S^2: (\mathcal{T}_1)_0^* &\rightarrow (\mathcal{T}_2)_0^*, & (p_2, p_5, p_6) &\mapsto (p_3, p_4, p_7), \\ (S^{-1}T)^2: (\mathcal{T}_1)_0^\diamond &\rightarrow (\mathcal{T}_2)_0^\diamond, & (q_2, p_9, p_{11}) &\mapsto (q_3, p_8, p_{10}), \end{aligned}$$

and

$$S^{-1}: \mathcal{O}_0^- \rightarrow \mathcal{O}_0^+, \quad (p_3, p_4, p_6, p_5, q_3, q_{14}, p_{13}, p_{15}) \mapsto (q_3, p_7, p_4, p_6, p_2, p_9, p_{11}, p_8).$$

Thus $S^{-1}(\mathcal{P}_{-1})$ and \mathcal{P}_+ are glued along \mathcal{O}_0^+ . According to Lemma 2.9, $S^{-1}(\mathcal{P}_{-1})$ lies in the interior of \mathcal{I}_0^+ , since \mathcal{P}_{-1} lies in the exterior of \mathcal{I}_0^+ . Moreover, $p_1 = S^{-1}(q_\infty) = [0, 0]$ is the center of the isometric sphere \mathcal{I}_0^+ ; see Figure 13. \square

Proposition 5.21 *Let Ω be the discontinuity region of Γ acting on $\mathbb{H}_{\mathbb{C}}^2$. Then the fundamental group of Ω/Γ has a presentation*

$$\langle u, v, w \mid w^{-1}vu^{-1}v^{-1}wu = v^2wuw^{-3}u = \text{id} \rangle.$$

Proof Let x_i for $i = 1, 2, 3, 4, 5, 6, 7, 8$ be the corresponding gluing maps of \mathcal{P} given in Lemma 5.20. These are the generators of the fundamental group of Ω/Γ .

By considering the edge cycles of \mathcal{P} under the gluing maps, we have the relations

$$\begin{aligned} x_7^{-1} \cdot x_5 \cdot x_7 \cdot x_1 &= \text{id}, & x_2^{-1} \cdot x_4 \cdot x_1 &= \text{id}, & x_2 \cdot x_3^{-1} \cdot x_4^{-1} \cdot x_6 \cdot x_1 &= \text{id}, \\ x_3^{-1} \cdot x_5^{-1} \cdot x_6 \cdot x_1 &= \text{id}, & x_2 \cdot x_3 \cdot x_2 &= \text{id}, & x_4^{-1} \cdot x_5 \cdot x_2 &= \text{id}, \\ x_7 \cdot x_8 \cdot x_6 &= \text{id}, & x_8 \cdot x_7 \cdot x_6 &= \text{id}, & x_8^{-1} \cdot x_7 &= \text{id}. \end{aligned}$$

For example, the edge cycle of $[q_\infty, p_2]$ is

$$[q_\infty, p_2] \xrightarrow{x_1} [q_\infty, p_3] \xrightarrow{x_7} [p_1, q_3] \xrightarrow{x_5} [p_1, p'_2] \xrightarrow{x_7^{-1}} [q_\infty, p_2].$$

Thus

$$x_7^{-1} \cdot x_5 \cdot x_7 \cdot x_1 = \text{id}.$$

This is the first relation. The others can be given by a similar argument.

Simplifying the relations and setting $u = x_1$, $v = x_2$ and $w = x_7$, we obtain the presentation of the fundamental group of Ω/Γ . □

Now we are ready to show the following theorem:

Theorem 5.22 *Let Ω be the discontinuity region of Γ acting on $\mathbb{H}_{\mathbb{C}}^2$. Then the quotient space Ω/Γ is homeomorphic to the two-cusped hyperbolic 3–manifold $s782$ in the SnapPy census.*

Proof Let $M = \Omega/\Gamma$. According to Proposition 5.21, the fundamental group of M has a presentation

$$\pi_1(M) = \langle u, v, w \mid w^{-1}vu^{-1}v^{-1}wu = v^2wuw^{-3}u = \text{id} \rangle.$$

The manifold $s782$ is a two-cusped hyperbolic 3–manifold with finite volume. Its fundamental group, provided by SnapPy, has a presentation

$$\pi_1(s782) = \langle a, b, c \mid a^2cb^4c = abca^{-1}b^{-1}c^{-1} = \text{id} \rangle.$$

Using Magma, we get an isomorphism $\Psi: \pi_1(M) \rightarrow \pi_1(s782)$ given by

$$\Psi(u) = c^{-1}b^{-1}, \quad \Psi(v) = b^{-1} \quad \text{and} \quad \Psi(w) = a.$$

Therefore M will be the connected sum of $s782$ and a closed 3–manifold with trivial fundamental group by the prime decompositions of 3–manifolds [15]. The solution of the Poincaré conjecture implies that the closed 3–manifold is the 3–sphere. Thus M is homeomorphic to $s782$. □

References

- [1] **M Acosta**, *Spherical CR Dehn surgeries*, Pacific J. Math. 284 (2016) 257–282 MR Zbl
- [2] **M Acosta**, *Spherical CR uniformization of Dehn surgeries of the Whitehead link complement*, Geom. Topol. 23 (2019) 2593–2664 MR Zbl
- [3] **A F Beardon**, *The geometry of discrete groups*, Graduate Texts in Math. 91, Springer (1983) MR Zbl
- [4] **M Culler**, **N M Dunfield**, **M Goerner**, **J R Weeks**, *SnapPy, a computer program for studying the geometry and topology of 3-manifolds* (2016) Available at <http://snappy.computop.org>
- [5] **M Deraux**, *On spherical CR uniformization of 3-manifolds*, Exp. Math. 24 (2015) 355–370 MR Zbl
- [6] **M Deraux**, *A 1-parameter family of spherical CR uniformizations of the figure eight knot complement*, Geom. Topol. 20 (2016) 3571–3621 MR Zbl
- [7] **M Deraux**, **E Falbel**, *Complex hyperbolic geometry of the figure-eight knot*, Geom. Topol. 19 (2015) 237–293 MR Zbl
- [8] **M Deraux**, **J R Parker**, **J Paupert**, *New non-arithmetic complex hyperbolic lattices*, Invent. Math. 203 (2016) 681–771 MR Zbl
- [9] **E Falbel**, *A spherical CR structure on the complement of the figure eight knot with discrete holonomy*, J. Differential Geom. 79 (2008) 69–110 MR Zbl
- [10] **E Falbel**, **P-V Koseleff**, **F Rouillier**, *Representations of fundamental groups of 3-manifolds into $\mathrm{PGL}(3, \mathbb{C})$: exact computations in low complexity*, Geom. Dedicata 177 (2015) 229–255 MR Zbl
- [11] **E Falbel**, **J Wang**, *Branched spherical CR structures on the complement of the figure-eight knot*, Michigan Math. J. 63 (2014) 635–667 MR Zbl
- [12] **W M Goldman**, *Complex hyperbolic geometry*, Clarendon, New York (1999) MR Zbl
- [13] **W M Goldman**, **J R Parker**, *Complex hyperbolic ideal triangle groups*, J. Reine Angew. Math. 425 (1992) 71–86 MR Zbl
- [14] **W M Goldman**, **J R Parker**, *Dirichlet polyhedra for dihedral groups acting on complex hyperbolic space*, J. Geom. Anal. 2 (1992) 517–554 MR Zbl
- [15] **J Hempel**, *3-Manifolds*, Ann. of Math. Stud. 86, Princeton Univ. Press (1976) MR Zbl
- [16] **J Ma**, **B Xie**, *Spherical CR uniformization of the magic 3-manifold*, preprint (2021) arXiv 2106.06668
- [17] **J Ma**, **B Xie**, *Menger curve and spherical CR uniformization of a closed hyperbolic 3-orbifold*, preprint (2022) arXiv 2201.04765

- [18] **J Ma, B Xie**, *Three-manifolds at infinity of complex hyperbolic orbifolds*, preprint (2022) arXiv 2205.11167
- [19] **GD Mostow**, *On a remarkable class of polyhedra in complex hyperbolic space*, Pacific J. Math. 86 (1980) 171–276 MR Zbl
- [20] **JR Parker**, *Notes on complex hyperbolic geometry*, University of Durham (2003) Available at <https://maths.dur.ac.uk/users/j.r.parker/img/NCHG.pdf>
- [21] **JR Parker, J Wang, B Xie**, *Complex hyperbolic $(3, 3, n)$ triangle groups*, Pacific J. Math. 280 (2016) 433–453 MR Zbl
- [22] **JR Parker, P Will**, *A complex hyperbolic Riley slice*, Geom. Topol. 21 (2017) 3391–3451 MR Zbl
- [23] **RE Schwartz**, *Degenerating the complex hyperbolic ideal triangle groups*, Acta Math. 186 (2001) 105–154 MR Zbl
- [24] **RE Schwartz**, *Ideal triangle groups, dented tori, and numerical analysis*, Ann. of Math. 153 (2001) 533–598 MR Zbl
- [25] **RE Schwartz**, *Complex hyperbolic triangle groups*, from “Proceedings of the International Congress of Mathematicians, II” (T Li, editor), Higher Ed. (2002) 339–349 MR Zbl
- [26] **RE Schwartz**, *Real hyperbolic on the outside, complex hyperbolic on the inside*, Invent. Math. 151 (2003) 221–295 MR Zbl
- [27] **RE Schwartz**, *A better proof of the Goldman–Parker conjecture*, Geom. Topol. 9 (2005) 1539–1601 MR Zbl
- [28] **RE Schwartz**, *Spherical CR geometry and Dehn surgery*, Ann. of Math. Stud. 165, Princeton Univ. Press (2007) MR Zbl
- [29] **JO Wyss-Gallifent**, *Complex hyperbolic triangle groups*, PhD thesis, University of Maryland (2000) MR Available at <https://www.proquest.com/docview/304626210>

*School of Mathematics, Hunan University
Changsha, China*

*School of Mathematics, Hunan University
Changsha, China*

*School of Mathematics, Hunan University
Changsha, China*

ypjiang@hnu.edu.cn, jywang@hnu.edu.cn, xiexbh@hnu.edu.cn

Received: 19 April 2021 Revised: 27 February 2022

ALGEBRAIC & GEOMETRIC TOPOLOGY

msp.org/agt

EDITORS

PRINCIPAL ACADEMIC EDITORS

John Etnyre
etnyre@math.gatech.edu
Georgia Institute of Technology

Kathryn Hess
kathryn.hess@epfl.ch
École Polytechnique Fédérale de Lausanne

BOARD OF EDITORS

Julie Bergner	University of Virginia jeb2md@eservices.virginia.edu	Robert Lipshitz	University of Oregon lipshitz@uoregon.edu
Steven Boyer	Université du Québec à Montréal cohf@math.rochester.edu	Norihiko Minami	Nagoya Institute of Technology nori@nitech.ac.jp
Tara E Brendle	University of Glasgow tara.brendle@glasgow.ac.uk	Andrés Navas	Universidad de Santiago de Chile andres.navas@usach.cl
Indira Chatterji	CNRS & Univ. Côte d'Azur (Nice) indira.chatterji@math.cnrs.fr	Thomas Nikolaus	University of Münster nikolaus@uni-muenster.de
Alexander Dranishnikov	University of Florida dranish@math.ufl.edu	Robert Oliver	Université Paris 13 bobol@math.univ-paris13.fr
Tobias Ekholm	Uppsala University, Sweden tobias.ekholm@math.uu.se	Jessica S Purcell	Monash University jessica.purcell@monash.edu
Mario Eudave-Muñoz	Univ. Nacional Autónoma de México mario@matem.unam.mx	Birgit Richter	Universität Hamburg birgit.richter@uni-hamburg.de
David Futер	Temple University dfuter@temple.edu	Jérôme Scherer	École Polytech. Féd. de Lausanne jerome.scherer@epfl.ch
John Greenlees	University of Warwick john.greenlees@warwick.ac.uk	Vesna Stojanoska	Univ. of Illinois at Urbana-Champaign vesna@illinois.edu
Ian Hambleton	McMaster University ian@math.mcmaster.ca	Zoltán Szabó	Princeton University szabo@math.princeton.edu
Matthew Hedden	Michigan State University mhedden@math.msu.edu	Maggy Tomova	University of Iowa maggy-tomova@uiowa.edu
Hans-Werner Henn	Université Louis Pasteur henn@math.u-strasbg.fr	Nathalie Wahl	University of Copenhagen wahl@math.ku.dk
Daniel Isaksen	Wayne State University isaksen@math.wayne.edu	Chris Wendl	Humboldt-Universität zu Berlin wendl@math.hu-berlin.de
Thomas Koberda	University of Virginia thomas.koberda@virginia.edu	Daniel T Wise	McGill University, Canada daniel.wise@mcgill.ca
Christine Lescop	Université Joseph Fourier lescop@ujf-grenoble.fr		

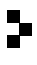
See inside back cover or msp.org/agt for submission instructions.

The subscription price for 2023 is US \$650/year for the electronic version, and \$940/year (+ \$70, if shipping outside the US) for print and electronic. Subscriptions, requests for back issues and changes of subscriber address should be sent to MSP. Algebraic & Geometric Topology is indexed by Mathematical Reviews, Zentralblatt MATH, Current Mathematical Publications and the Science Citation Index.

Algebraic & Geometric Topology (ISSN 1472-2747 printed, 1472-2739 electronic) is published 9 times per year and continuously online, by Mathematical Sciences Publishers, c/o Department of Mathematics, University of California, 798 Evans Hall #3840, Berkeley, CA 94720-3840. Periodical rate postage paid at Oakland, CA 94615-9651, and additional mailing offices. POSTMASTER: send address changes to Mathematical Sciences Publishers, c/o Department of Mathematics, University of California, 798 Evans Hall #3840, Berkeley, CA 94720-3840.

AGT peer review and production are managed by EditFlow[®] from MSP.

PUBLISHED BY

 **mathematical sciences publishers**
nonprofit scientific publishing

<http://msp.org/>

© 2023 Mathematical Sciences Publishers

ALGEBRAIC & GEOMETRIC TOPOLOGY

Volume 23

Issue 9 (pages 3909–4400)

2023

Two-dimensional extended homotopy field theories	3909
KÜRŞAT SÖZER	
Efficient multisections of odd-dimensional tori	3997
THOMAS KINDRED	
Bigrading the symplectic Khovanov cohomology	4057
ZHECHI CHENG	
Fibrations of 3–manifolds and asymptotic translation length in the arc complex	4087
BALÁZS STRENNER	
A uniformizable spherical CR structure on a two-cusped hyperbolic 3–manifold	4143
YUEPING JIANG, JIEYAN WANG and BAOHUA XIE	
A connection between cut locus, Thom space and Morse–Bott functions	4185
SOMNATH BASU and SACHCHIDANAND PRASAD	
Staircase symmetries in Hirzebruch surfaces	4235
NICKI MAGILL and DUSA MCDUFF	
Geometric triangulations of a family of hyperbolic 3–braids	4309
BARBARA NIMERSHIEM	
Beta families arising from a v_2^9 self-map on $S/(3, v_1^8)$	4349
EVA BELMONT and KATSUMI SHIMOMURA	
Uniform foliations with Reeb components	4379
JOAQUÍN LEMA	